CHAPTER 5
SURFACE CHEMISTRY IN FILTRATION

5.1 INTRODUCTION

5.1.1 Background

The production of fine particles has arisen as a result of technological changes and product requirements in mining, metallurgical, ceramics, paper, food and chemical industries. The fine grinding is also necessary to make high quality micro/nano scale materials. It is well known that the fine particles are difficult to dewater using the existing dewatering techniques, such as vacuum, pressure, and centrifugal filtrations [1-3]. Accordingly, the dewatered products have high moisture content, which often necessitates the use of thermal dryers. These are the only methods to reduce the moisture content to desired levels. However, thermal drying is a costly method and creates environmental pollution where the operation is located. Therefore, it is a major concern to decrease the moisture content of the final product that will be delivered to thermal driers (e.g., rotary, fluidize bed and flash) and to obtain significantly low moisture [4-7].

Coarse particles compared to fine particles have lower surface area and larger capillary radius that results high filtration rates and low moisture contents. High surface moisture in the cake entails high transportation and dewatering costs, handling and storage problems, corrosion in combustion chambers of thermal power stations, surface oxidation, negative effects on the metallurgical coke production, freezing in the cold climate, penalties for British Thermal Unit (BTU) loss in product, leaching of the sulfide minerals, etc. [2,5,8-12]. It is therefore necessary to develop advanced dewatering technologies that can help solve the problems associated with the processing of the fine particles.

To address the problem, two new dewatering technologies have been developed at Virginia Tech for fine particle dewatering. The first is a novel dewatering aid using low hydrophile-lipophile balance (HLB) surfactants that can substantially improve the mechanical dewatering processes. The second is a centrifugal dewatering technique that is a combination of centrifugal force and air/vacuum pressure in one single unit. A more specific explanation of the novel centrifuge method was given in Chapter 3. In this Chapter, surface chemistry of fine particles is communicated in detail, and its effects on the moisture content, dewatering kinetics,

and cake parameters are evaluated in the absence and presence of the novel dewatering chemicals.

As explained in the previous Chapters, four different types of the *novel reagents* were developed and used on fine coal and mineral particles. These are mainly non-ionic low HLB surfactants including pure reagents (fatty acid, fatty esters, phosphate esters, hydrophobic polymers, etc), hydrophobic polymer, lipids and modified lipids. Some of the chemicals used as dewatering aids are insoluble in water, so they are dissolved in appropriate carrier solvents using light hydrocarbon oils (kerosene, diesel, etc) and short-chain alcohols whose carbon atom numbers are less than eight [13-18].

It is stated that use of the novel chemicals improve the contact angle closer to or above 90° where the wetability is ended and capillary radii, and reduce the surface tension of the filtrate. In addition to polymer, electrolytes or coagulants, the dewatering aids cause particles to coagulate by virtue of increased particle hydrophbicity. As a result, the efficiency of dewatered fine particles and dewatering kinetic are greatly increased [2,13,18].

The surfactants are added to the slurry to increase the hydrocarbon chain density (or formation of the surface coverage) onto the particle surface. Therefore, particle hydrophobicity increased by the chemicals cause to liberate the water on the surface (or in capillary tubes). Afterwards, it is easily removed during the air/vacuum operation [15-21]. This concept is particularly important for the dewatering processes presented in these studies.

<u>*Laplace Equation*</u>: According to this equation, it is well known that the water in the capillary tubes shown in Figure 5.1 can be removed since the applied pressure is larger than the capillary pressure, p:

$$p = \frac{2\gamma_{23}\cos\theta}{r} \quad , \qquad [1]$$

where r is capillary radii, γ_{23} are the surface tension of the liquid, and θ is the air-water-solid interface contact angle. It is seen that p decreases with decreasing $\gamma_{23,}$ increasing θ and r at contact angle lower than 90° [5,9,19,20]. However, if the contact angle is higher than 90°, the capillary pressure will be negative in the tubes. In order to increase the negative capillary pressure of the tubes, it is necessary to increase the surface tension of the liquid and decrease the

capillary radii. For the changes in the capillary pressure as a function of these variables, a simple computer program has been developed in Mathematica and given in the Appendix J.

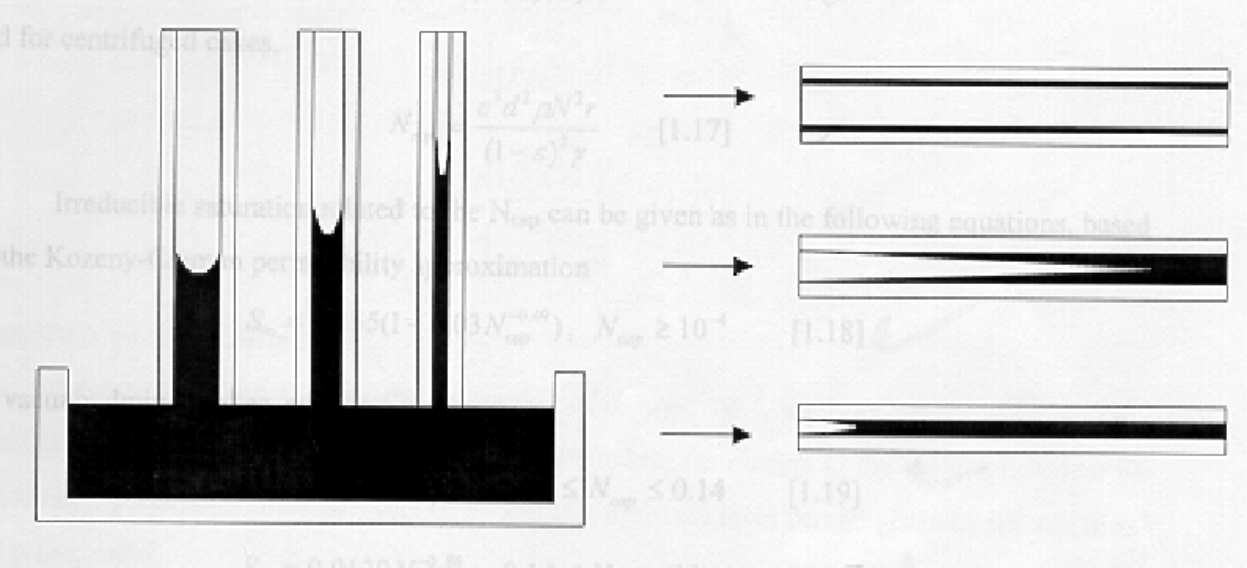

a) Vertical capillary b) Horizontal capillary

Figure 5.1 Effects of the capillary diameters on the formation of capillary forces

HLB numbers: These are useful parameters for understanding several surface and colloid chemistry processes including emulsion formation, wetting/dewetting, hydrophobic coagulation, etc [11,14,15,18]. It has been determined that when charges of the surfactant heads are of the same sign as coal or mineral particles, the polar head of the surfactants will be repelled from the surface due to the electrostatic repulsion forces. This increases the tendency for the polar heads to point toward the liquid phase, thereby, promoting the inverse orientation on the solid surface. Such orientation makes the surface hydrophilic (or wettable surface) owing to the oxygen compounds of the surfactant head groups. It is a known fact that the head of the surfactant usually attracts water molecules and keeps more water on the surface, which is not desired in the chemical dewatering process [11,25,14-20]. The surfactants with higher HLB numbers generally conform to this tendency. However, Yoon et al reported that low HLB (<15) surfactants used as dewatering aids could not have this tendency [22]. These surfactants could be added to ~~a~~ slurry to simultaneously decrease the liquid-vapor interface surface tension and increase the contact angle and capillary radius [2,5,13,25]. As shown, the surfactant tails that align through the aqueous media expel the water molecules from the particle surface due to the hydrophobicity of

the tails and as a result the surface becomes non-wettable.

The HLB numbers are essentially a measure of the hydrophilicity of a surfactant, and they vary with molecular structure. This number can also represent the solubility of the surfactant in water. For example high HLB surfactants can be more soluble. Hence, if the surfactant structure is known, it should be possible to determine its HLB number. According to Davies and Rideal, HLB numbers can be found by the following equation [21,22]:

$$HLB = \Sigma(\text{Hydrophilic group numbers}) + \Sigma(\text{Lipophilic group numbers}) + 7, \quad [2]$$

Table 5.1 and Table 5.2 list various HLB group numbers and the HLB numbers of commercially used surfactants, respectively [18].

Table 5.1 HLB numbers of hydrophilic and lipophilic groups

Hydrophilic Groups	HLB	Lipophilic Groups	HLB
$-SO_4Na$	38.7	-CH-, $-CH_2-$,	-0.475
-COONa	19.1	$-CH_3-$, -CH=	-0.475
-N (tertiary amine)	9.4		
Ester (sorbitan ring)	6.8	$-(CH_2- CH_2- CH_2-O-)$	-0.15
-COOH	2.1		
-OH (free)	1.9		
-O	1.3		

Table 5.2 HLB numbers of selected commercial surfactants

Surfactants	Commercial Name	HLB Numbers
Sodiumdodecylsulfate	-	40
Sodiumdodecylsulfosuccinate	Aerosol	35.3
Sodium Oleate	-	18
Amine, ethoxylated	Tomah E-18-15	16
Polyoxyethylene sorbitan monooleate	Tween 80	15
Sorbitan monooleate	Span 80	8.6
Polyoxyethylene (2) cetyether	Brij 52	5.3
Cetylalcohol	-	1.3
Oleic Acid	-	1

The HLB numbers are also used for selecting suitable emulsifying surfactants for different oils. Bancroft [23] suggests that the liquid in which an emulsifying agent is more soluble becomes a continuous phase. Thus, hydrophilic surfactants are used for producing oil-in-water (O/W) emulsions, while hydrophobic surfactants are used for producing water-in-oil (W/O) emulsions [18,23,24].

5.1.2 Thermodynamics of Dewatering

For the thermodynamic criteria, Gibbs free energy ΔG (joules) is usually preferred to use for several processes. When the free energy change of a system is lower than zero, the process is thermodynamically favorable. In order to obtain a negative ΔG value, enthalpy ΔH is minimized, while the entropy ΔS (joules/°C) is maximized for a given system. Generally, the free energy of the system can be given below [4,5,11,14-18,20]:

$$\Delta G = \Delta H - T\Delta S \quad [3]$$

where T is absolute temperature (K). Note that for the adsorption of polymer on a solid surface, the entropic adsorption may be more dominant; however, for the surfactant adsorption, enthalpic adsorption may be more important [11,14-20].

a) Displacement of Water

When a solid particle is immersed in water, the water molecules adsorb on the surface depending on the hydropobicity of the particles. It was expressed that the Laplace equation could be used for the dewatering of the fine particle in which a bundle of capillary tubes existed. In addition, Yoon et al suggests that the thermodynamics of dewatering process may be shown by Figure 5.2, in which a particle **1** is emerged from water **3** into air **2** phases [2,9,23,25,42]. In this model, it is seen that the process is focused on a single particle. During this process, a change of the free energy per unit surface area of particles can be given by the following relationship:

$$\frac{dG_{dis}}{dA} = \gamma_{12} - \gamma_{13} \quad [4]$$

where γ_{12} is interfacial tension between the particle and air and γ_{13} is the same tension between the particle and water. During the air/vacuum pressure on the cake, the solid/water interface is displaced by solid/air interface to receive dryer filter product.

According to Figure 5.2 b, the Young`s equation can be stated as a function of water contact angle (θ) and the interfacial surface tensions (or energies) between the components (γ_{12}, γ_{13} and γ_{23}) at which they are equilibrium:

$$\gamma_{12} - \gamma_{13} = \gamma_{23} \cos\theta \quad [5]$$

Substituting Equation [5] into Equation [4], one can obtain the following relationships:

$$\frac{dG_{dis}}{dA} = \gamma_{23} \cos\theta < 0 \quad [6]$$

For a dewatering process, the value of dG_{dis}/dA should be less than zero (or contact angle should be higher than 90°), which may be a thermodynamic criterion for the spontaneous dewatering. Similar observation can be seen in the Laplace equation due to the cosθ component in the formula, i.e., at θ > 90 [2,42].

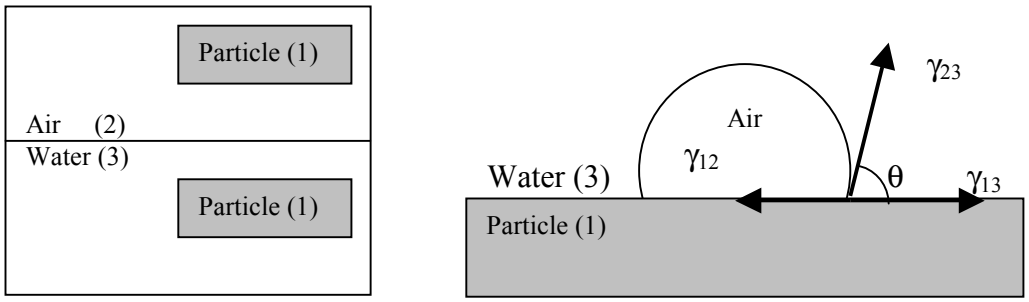

Figure 5.2 a) A schematic representation of dewatering process, b) equilibrium contact angle between three interfacial tensions.

However, even the most hydrophobic particles (bituminous coal, sulfur, molybdenum and talc minerals) have water contact angles far less than 90°. Aplan [43] determined that the contact angles of the best bituminous coal samples were less than 70°, and the average contact angle values are around 40_s°. As seen, this condition cannot be met for the spontaneous dewatering. Therefore, mechanical filtration of untreated particles is not a thermodynamically favorable process for the chemical dewatering [2,9,18,42,43-48].

According to the Equations [1] and [6], the surface tension of liquid and contact angles of a solid should be controlled for the mechanical dewatering. These components will decrease the value of the surface energy (or free energy) that could be equivalent to reducing the energy barrier (or activation energy) for the spontaneous dewatering. This conceptual energy barrier can be overcome by various energy inputs, such as air/vacuum pressure, G-force or electrolyte additions. In addition to these, if one adds a volume of surfactant to the slurry in order to decrease surface tension of the liquid and increase the contact angle, this energy barrier may be overcome, as well [2,42,49-55].

b) Hydrophobic Forces

Even though a number of mechanisms of the hydrophobic forces have been suggested in the literature, none of which have not been accepted so far. These include water structure effects, metastability of the film, electrostatic mechanisms, for the hydrophobic forces, cavitation effects

and other mechanisms [11,17,18,56,57,73,74]. It was also stated that hydrophobic forces could be divided into two major forces: short-range hydrophobic force and long-range hydrophobic force. Since the beginning of the 1990s, long-range hydrophobic force studies have been conducted on several material surfaces prepared using a variety of methods. These are in situ equilibrium adsorption, Langmuir-Blodgett (LB) film deposition, and chemical modification of the surfaces and equilibrium adsorption of surfactant on the solid surface. It has been shown that the long-range force is dependent mostly on the hydrophobicity of the surface [11,17,18].

Since Isrealachivili and Pashley first measured the hydrophobicity in 1982 [56,57], several investigators have focused on this concept to solve the driving force of many surface chemistry and biochemistry related processes [17,18,58-66]. Yoon et al reported that there exists a relationship between the hydrophobic force and the contact angle using atomic force microscopy (AFM) to solve the mechanisms of flotation and coagulation processes [61-66].

In addition, the basis of chemical dewatering is to control the hydrophobicity of the fine particles to be dewatered. The most widely used technique for the hydrophobicity is the water contact angle at air/water/solid interface. The contact angle is a thermodynamic property, and it only predicts the spontaneity of the dewatering, flotation, coagulation, agglomeration and colloid chemistry processes [17,18,63-69]. In the present work, the contact angle and hydrophobicity relationship will be explained in the following sections.

Extended DLVO Theory: It is pointed out that if the contact angle is larger than 40°, the classical DLVO theory cannot fit with the experimental results; therefore, it is necessary to extend the DLVO theory by combining a hydrophobic force term F_h, which is not considered in the classical DLVO theory. The extended DLVO theory at the larger contact angle may be expressed as [17,62,65-69]:

$$F = F_e + F_d + F_h, \qquad [7]$$

at which F_e is electrostatic repulsive force and F_d is London wan der Waals force. The hydrophobic force term can be written when θ is 60° or over:

$$\frac{F_h}{R} = C_0 \exp\left(\frac{-H}{D_0}\right) \qquad [8]$$

where R is the radius of curvature of spherical object, H is separation distance. When a strong hydrophobic force exists between two surfaces due to the higher contact angle (over 90°), a double-exponential function can be used to measure accurate surface forces [61-68].

$$\frac{F_h}{R} = C_1 \exp\left(\frac{-H}{D_1}\right) + C_2 \exp\left(\frac{-H}{D_2}\right) \quad [9]$$

where C_0, C_1 and C_2 are related to interfacial tension at the solid/liquid interfaces and D_0, D_1 and D_2 are referred as decay lengths. If the hydrophobic force is weak, D_2 is zero, while the values of D_1 is in the range of 1 to 1.3 nm. However, when the hydrophobic force is strong, D_2 becomes significantly higher (2 to 35 nm) at contact angle over 90°. This may suggest that dewatering can become spontaneous by displacing water molecules by air phase. Equation [9] can also be described as a power law [61-68].

$$\frac{F_h}{R} = \frac{-K}{6H^2} \quad [10]$$

in which the constant K is the only fitting parameter for a force curve. This equation is the same form as the well-known van der Waals attraction force. Thus, K value can be compared with the Hamaker constant A. More detailed information was given in Chapter 1 about K value [61-64].

c) Acid-Base Interactions

For over 30 years, the thermodynamic treatment of a surface has been made to control the free energy components, which is beneficial for many surface processes. Fowkes, Zisman, Laskowski and Kitchener, Israelachvili and Pashley, van Oss, Chaudhary and Good have done the pioneering works on the surface treatment processes [70-74]. According to the later authors` approaches, the surface free energy γ_i of a phase can be expressed:

$$\gamma_i = \gamma_i^{LW} + \gamma_i^{AB}, \quad [11]$$

at which γ_i^{LW} is the Lifshitz van der Waals interaction including London dispersion, Debye induction and Keesom dipole-dipole interactions and γ_i^{AB} is the acid-base interaction:

$$\gamma_i^{AB} = 2\sqrt{\gamma_i^+ \gamma_i^-} \quad [12]$$

where γ_i^+ and γ_i^- refer to the electron acceptor (or Lewis acid) and electron donor (or Lewis base). These parameters are the contribution of the acid-base free energy of the phase *i*.

When two phases (solid and liquid) exist in a system, one can drive the following equation [17,73]:

$$(1 + \cos\theta)\gamma_{lv} = 2(\sqrt{\gamma_s^{LW} \gamma_l^{LW}} + \sqrt{\gamma_s^+ \gamma_l^-} + \sqrt{\gamma_s^- \gamma_l^+}), \quad [13]$$

which is the most relevant equation in determining surface free energy components of solids or liquids (γ_i^{LW}, γ_i^+ and γ_i^-) without using a microcalorimeter. In order to obtain the surface tension values, contact angle measurements of three different known solids or liquids should be conducted on each sample. By solving three equations with three unknowns, the sample parameters can be determined for the further predictions [61-65,17,73]. More detailed information was given in Chapter 1 about acid-base interactions.

When the surface tension of a liquid (or surfactant) is lower than that of a solid, the liquid will spread on the surface (i.e., $\theta=0°$); therefore, it is not possible to measure contact angles. To get around this problem, contact angle measurements were conducted in water rather than in air so that non-zero contact angles could be obtained. In the present work, a syringe was used to place a small droplet of a reagent (dewatering aid) on the surface of a solid, which was immersed in water. In using Eq. [13], the liquid-air surface interfacial (γ_{lv}) was substituted by the liquid-water interfacial tension (γ_{wr}). In the present work, the values of (γ_{wr}) were determined using the Fowkes equation:

$$\gamma_{wr} = \gamma_w + \gamma_r - 2\sqrt{\gamma_w^d \gamma_r^d}\,, \qquad [14]$$

in which γ_w is water-air surface tension, γ_r is reagent-air surface tension, γ_w^d is dispersion energy of water and γ_r^d is that of the reagent. The value of γ_r^d was determined from the contact angle of the reagent measured on the surface of a Teflon plate [17,18] using the following equation:

$$(1 + \cos\theta)\gamma_{rv} = 2(\sqrt{\gamma_s^d \gamma_r^d}\,), \qquad [15]$$

which is a reduced form of Equation [13] for non-polar solids such as, Teflon.

5.1.3 Kinetics of Dewatering

For over 100 years, several models have been developed for predicting the dewatering mechanisms of the filter cake during the vacuum or air pressure operation [24-38]. These models (or semi-empirical models) are mostly based on the rate of fluid flow, cake saturation, cake permeability, cake and medium resistance, surface tension, viscosity, Reynolds number, cake throughput, air flow, pressure drop across the bed, residual moisture in the cake, etc. However, the Darcy model [38] is the most widely accepted one, and has been used for almost 150 years. In addition, in the 1970s, Wakeman developed a dewatering model that was also widely accepted

by filtration experts. This model can only predict i) equilibrium saturation at a given pressure, ii) desaturation profile with time and iii) air flow necessary for the desaturation of the cake. Note that the dewatering parameters associated with equilibrium dewatering conditions are important issues for understanding the behavior of the cake during the filtration process [28-35].

Generally, dewatering is achieved by displacing filtrate with the applied forces, e.g. vacuum/air pressure, cyclone and centrifugal forces. In the first stage of the dewatering process, a cake is formed on the filter media, and then the wetting liquid flows through the cake [5,13,28,29]. This liquid flow can be described by the Darcy`s law [38-41]:

$$\frac{dV}{dt} = \frac{\Delta p A^2}{\mu(wVR + AR_f)} \qquad [16]$$

where dV/dt is the rate of filtrate flow, Δp is vacuum pressure differential, μ is dynamic viscosity of filtrate, A is the filter cake area, w is weight of the dry solids per unit volume of filtrate, R is specific cake resistance and R_f is specific filter medium resistance. By integrating Equation [16] and rearranging, one can obtain a well-known filtration equation [13,28,29,39-41]:

$$\frac{t}{V} = (\frac{\mu wR}{2\Delta pA^2})V + \frac{\mu R_f}{\Delta pA} \qquad [17]$$

at which V is the volume of the filtrate and t is filtration time. Using a laboratory apparatus (graduated cylinder or electronically volume measurable device), the slurry can be dewatered and the volume of filtrate versus filtration time can be obtained. The later equation is of a straight line form, e.g. y = mx + b. Therefore, plotting the t/V values on y-axis and the V values on x-axis will result in a straight line for the cake and medium resistance. The slope of the line will be the same as $\mu wR/2\Delta pA^2$, so the specific cake resistance R can then be found for the further cake parameters. Meanwhile, the intercept of the same line on the y-axis will give the specific resistance of the filter media R_f using the term $\mu R_f/\Delta pA$.

From the cake resistance value, the following parameters, such as cake permeability K, Kozney mean diameter d_k, breakthrough pressure P_b and equilibrium pressure S_e can also be calculated using the appropriate equations given below [5,13,28,29,39-41]:

$$K = \frac{1}{R\rho_c(1-\varepsilon)} \qquad [18]$$

which is known as cake permeability [39-41]. The sign ρ_c is specific density of coal and ε is cake porosity, which is dependent on the particle size. The cake porosity can be written:

$$\varepsilon = \frac{v_0}{V + v_0} \quad [19]$$

where V and v_0 are volume of the solid and void space, respectively.

The Kozney mean diameter d_k, which is related to the capillary tubes in the filter cake, is also proportional to the cake permeability:

$$K = \frac{\varepsilon^3 d_k^2}{150(1-\varepsilon)^2} \quad [20]$$

The effect of varying pressure drop across the filter cake is a major parameter for vacuum filtration. Since the applied pressure is higher than the capillary pressure, dewatering will spontaneously continue by displacing the water from the voids. Carleton and Mackay defined that a minimum pressure required to remove the water, which is also called breakthrough pressure P_b [41]:

$$P_b = \frac{\alpha\gamma\cos\theta(1-\varepsilon)}{d_k\varepsilon} \quad [21]$$

where γ is filtrate surface tension, θ is solid/air/water contact angle and α is breakthrough pressure constant. It was found 4.6 for sand particles [28,29] and 0.83 fine coal particles [39-41].

The equilibrium saturation S_e that is the saturation of the cake at infinite time can be shown as:

$$S_e = S_\infty + (1- S_\infty)\left(\frac{p_b}{\Delta P}\right)^\lambda \quad [22]$$

at which λ is pore size distribution index, S_∞ is irreducible saturation and ΔP is vacuum pressure. It was reported that λ was 0.7 for coal and 5 for sand, which is not a constant number [28,29,39].

In the practice, moisture in the cake cannot be totally removed by chemical-mechanical filtration due to the complexity of the cake structure. Thus, Wakeman described a model to figure out the irreducible saturation S_∞ [28-35]:

$$S_\infty = 0.155(1+0.031\ N_{cap}^{-0.49}) \quad [23]$$

where N_{cap} is the capillary number. This number changes with the filtration methods. For vacuum filtration:

$$N_{cap} = \frac{\varepsilon^3 d^2(\rho g L + \Delta P)}{(1-\varepsilon)^2 L\gamma}, \qquad (10^{-5} < N_{cap} < 0.14) \quad [24]$$

at which g is gravitational acceleration, d is particle diameter, L is cake depth and γ is surface tension. At the end of drying cycle time when the dewatering is completed, some moisture remained in the cake is called residual saturation S_R:

$$S_R = \frac{S - S_e}{1 - S_e}, \qquad [25]$$

where S is cake saturation, which corresponds with the final moisture content in the cake. It was also reported that this value could be changed because of the dewatering and particle conditions [5,28,29,39-41].

5.2 EXPERIMENTAL

5.2.1 Materials

Several DMC samples including Pittsburgh No 8, Elkview-Canada, Middle Fork-Virginia and Massey-West Virginia were tested for surface characterization and dewatering kinetic tests. In the characterization study, coal samples were prepared for image, surface area, zeta potential, and atomic composition tests. In the kinetics tests, the samples were crushed, ground and floated using kerosene as collector and MIBC as frother before tests. When the flotation tests were conducted, the samples were used within a few days to overcome the superficial oxidation and other contaminations. In addition, silica powder (0.038 mm x 0) obtained from Fisher Chemical was used for electrokinetic and dewatering tests.

The same samples were also used to determine the contact angle and acid-base components of the solid. In order to determine the acid-base components of the coal sample, nano-pure water and HPLC-grade glycerol and methyleniodide from Aldrich Chemical Company were employed for the contact angle measurements. For the liquid (dewatering aid) components, three known solids (teflon, mica and glass plate) were chosen for each liquid. The teflon and glass plates were cleaned in a boiling nitric acid solution for 12-14 hours to eliminate any surface contamination before use. However, the mica sample was carefully peeled to obtain a clean and smooth surface.

5.2.2 Apparatus and Procedure

Surface Imaging Analysis: The analysis of the coal surfaces was conducted using a Leitz Orthoplan Reflection Light Microscopy (LORLM) connected to a Pixera Camera. This

microscopy can determine nano/micron size minerals, such as pyrite, markacite and other organic and inorganic matters on the coal surface. Before the image tests, different coal samples were polished using different sized sand papers (120, 240, 400 and 600 grit) and then a polishing cloth was used with a 0.05 μm alumina micro polisher in order to obtain a smooth surface. The coal surfaces were then imaged to find out the markacite and pyrite minerals.

Surface Area Measurement: The surface area is one of the most important parameters for surface chemistry. The surface area of particles is usually determined using a technique (BET), which relies on the adsorption of gases on the particle surface at a low temperature. The mass of the gas adsorbed on the surface is measured as a function of the applied gas pressure under the liquid nitrogen atmosphere. Based on the gas pressure, the nitrogen gas makes a mono- or multy-layer on the surface. Using an appropriate formula, the surface area of the particles can be found [5,13,18]. For the surface area tests, two coal samples were crushed, grounded and subjected to the BET (NOVA 1200, version 6.08 High Speed Gas Sorption Analyzer) tests.

Zeta (ζ) Potential Measurements: The tests were conducted on the coal and silica powder samples using a Pen Kem Model 501 Laser Zeta Meter. The suspension was prepared by dispersing 0.1 grams of -38 μm sample in 500 ml nanopure water in the presence and absence of aluminum sulfate ($Al_2(SO_4)_3.18H_2O$). The pHs of the slurry was adjusted using diluted NaOH and HCl solutions. For each pH value, at least three ζ-potential measurements were read and the results were averaged.

XPS Analysis: It is described as a monoenergetic x-ray ejecting electrons from various atomic levels to determine atomic compounds of a surface with approximately 5 nm in depth. The percentages of the elements on the surface are between 96% and 99%. It is mostly used for the surface composition and oxidation levels of the substances [14-19,104]. In these tests, a Parkin-Elmer PHI 5400 model XPS spectrometer was used to determine the surface composition of coal samples. The x-ray scan size of the unit on the sample is 1 x 3 mm in size. In order to determine the surface compositions, the Pittsburgh and Middle Fork coal samples (1 x 1 cm) were polished to receive fresh surfaces before the tests.

Contact Angle Measurements: The tests were performed using a Rame Hart Model 100 Goniometer and Sigma70 technique. In the previous measurements, the sessile liquid drop technique was chosen to measure the advancing contact angle (θ_a) on the solid samples as suggested by van Oss and Good [17,94]. The surfaces of the coal specimens were polished as

explained above. To be able to eliminate experimental errors, a small 5 ml size syringe with a needle was utilized during the tests. The contact angle values were then used to determine the acid-base components of the coal samples [17,18,73,74].

Four different reagents, namely TDDP, ROE, Span 80 and SBO dissolved 33.3% in diesel oil were selected to find out the acid-base parameters of the liquids. First of all, surface tensions of the liquids were measured using a ring method of the Sigma70 measurement technique. The contact angle measurements of the mica and glass samples were then carried out using the liquids in nanopure water due to the spreading of reagents on the surface into the air.

AFM Measurements: For surface force measurements, Digital Instruments Nanoscope III type AFM in a manner described by Rabinovich and Yoon [61] were conducted on clean smooth silica plates obtained form Haraeus Amersil, Inc., and glass spheres obtained form Duke Scientific. Standard triangular silicon nitride (Si_3N_4) and SPM cantilevers on which a glass sphere was attached by means of Epon R Resin 1004F from the Shell Company were used for the measurements. All experiments were carried out using conductivity water (18.1 MΩ) produced by a Barnstead Nanopure II water treatment device. High purity dodecyleamine hydrocloride (DAHCl) received from Aldrich Chemical Company was used for the initial surface hydrophobization of the silica plates. AFM measurements were then conducted on the plates with the addition of the dewatering aids.

In addition, several other tests were conducted on the samples to confirm the reagent adsorption on the hydrophobic surfaces. For this reason, silica plates were coated by graphite using *PLD* technique, which is a physical vapor deposition process. The tests were carried out at $5.5x10^{-5}$ torr vacuum pressure and room temperature (~25°C). The thickness of the carbon film, which is mostly diamond like carbon, was approximately 50 nm. The coated plates were then introduced to the *LB* film deposition unit to determine the surface coverage or surfactant film formation on the surface.

Dewatering Kinetics Studies: The experiments were performed using an apparatus shown in Figure 5.3. A measured volume of slurry was poured into the pressure filter explained in Chapter 2, and then applying air pressure formed the cake. During the cake formation time, the filtrate was simultaneously transferred to a cylindrical tube consisting of a pressure transducer at the bottom of the cylinder. The transducer was connected to a PC to electronically measure the

volume of the filtrate versus time. The obtained data was then converted into time/volume as a function of filtrate volume to predict the cake parameters.

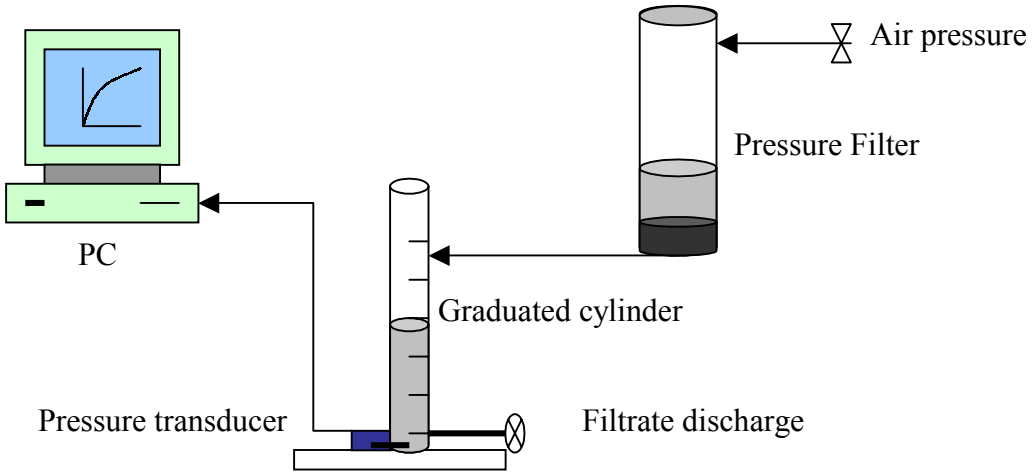

Figure 5.3 Schematic representation of kinetic test apparatus and test set-up

5.3 RESULTS AND DISCUSSIONS

5.3.1 Characterization of the Coal Samples

Surface Imaging Analysis: The primary objective of this study was to determine the iron sulfides on the coal surface, which affects the surface oxidation of the coal particles in an aqueous media. When the particles are oxidized, the surface becomes more hydrophilic due to the hydroxyl spices on the surface. These phenomena can decrease the surfactants adsorption on the coal surface and give low moisture reduction in the cake. Not only that, sometimes moisture content of the cake is increased depending on the oxidation levels of the surface. In order to determine the sulfide minerals on the coal surface, several LORLM image tests were conducted on the polished Pittsburgh and Elkview coal samples.

Figure 5.4 shows the image analysis of Pittsburgh and Elkview coal samples. The test results revealed that the coal surfaces consisted mainly of different coal macerals, sulfide and clay minerals. However, a more striking observation was seen on the Pittsburgh coal sample, because it had both pyrite and markacite minerals on the surface. It was found that the markacite minerals quickly reacted with water molecules and made the coal surface more hydrophilic due to the high oxygen affinity of the markacite mineral [4,16,47]. In other words, ferric hydroxyl spices formed on the surface. Therefore, these coal samples cannot be dewatered for a longer

time in the plants. These explanations are also identical to the dewatering test results given in Chapter 2 and Appendices. However, the Elkview coal samples have only pyrite minerals, and the surface oxidation can be lower than the other coal. This is why the Elkwiev coal sample can be dewatered longer time in the laboratory conditions.

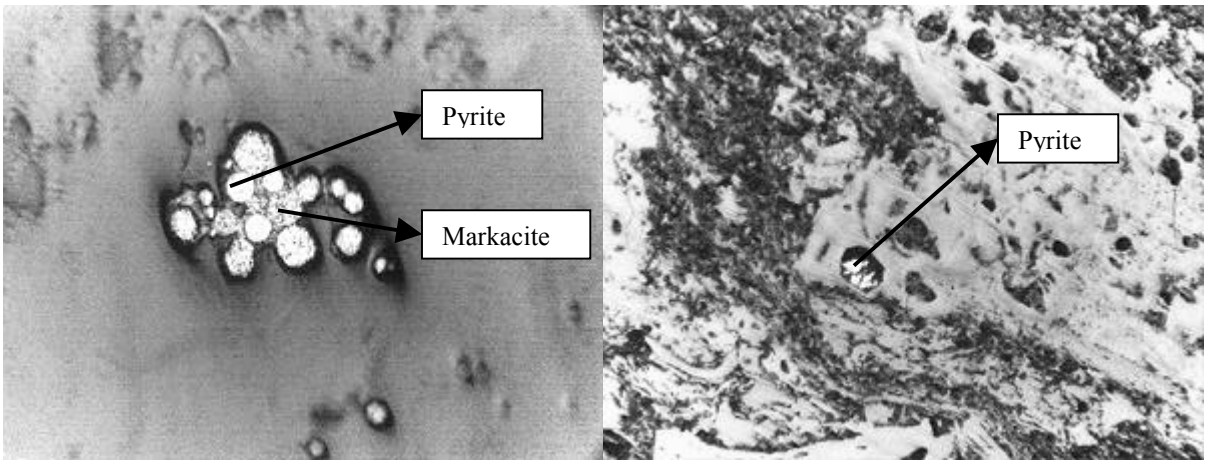

a b

Figure 5.4 LORLM image analysis of a) Pittsburgh No: 8 coal sample and b) Elkview-Canada coal samples (0.4 x 0.3 mm)

Table 5.3 Effects of time on the coal samples* in water

Changes on the samples	Coal Samples	
	Pittsburgh	Elkview
Water pH[1]	5.58	6.54
Water Color	Yellow-Brown	No Change
Contact angle (Fresh/Aged)	46/24	47/40
[2]Moisture Content (Fresh/Aged)	20.4/23.6	18.6/19.8

* The samples (0.5 mm x 0) floated using 1 lb./ton kerosene and 100 g/ton MIBC;[1] initial pH of water 6.82; [2] base tests moisture contents

In order to prove the assumptions, a series of tests were conducted on the Pittsburgh and Elkview coal samples. After two days of aging in water, the pH, color of the water, contact angles and base line moisture contents were measured on each sample. The test results given in Table 5.3 indicate that the changes of the pH, watercolor, contact angles and moisture contents on the Pittsburgh coal were higher than that of the Elkview coal samples. This could be due to the fact that the Pittsburgh coal contained a large amount of markacite, which oxidize and render the coal hydrophilic.

Surface area analysis: To better understand the relationship between the surface area and surface coverage by the surfactant molecules, a set of BET tests using NOVA 1200, version 6.08 High Speed Gas Sorption Analyzer were conducted on the fine Pittsburgh coal (0.1 mm x 0) and West Virginia coal (1 mm x 0) samples. The test results indicated that the Pittsburgh and West Virginia coal samples consisted of 1.09 m^2/g and 0.044 m^2/g surface areas. It is expected that the higher surface area sample needs a larger volume of surfactant to make the particles hydrophobic enough for the dewatering processes [5,11-19]. According to the BET results, it is clear that the Pittsburgh coal sample needs more reagent than the other sample for efficient dewatering.

Table 5.4 Effects of surface area on dewatering of Pittsburgh and West Virginia coal sample* using Span 80 at 100 kPa pressure

Reagent Dosages (lb/ton)	West Virginia Coal (0.044 m^2/g)		Pittsburgh Coal (1.09 m^2/g)	
	Surface Coverage (%)	Moisture Content (%)	Surface Coverage (%)	Moisture Content (%)
0	0.00	19.7	0.00	28.4
1	805.2	11.0	32.5	23.9
2	1610.4	10.8	65.0	20.4
3	2415.6	10.3	97.5	16.2
5	4026.0	9.8	162.5	14.3

* 2.5 in diameter air pressure filter used; the samples floated using 1 lb/ton kerosene and 100 g/ton MIBC; solid content of samples 17%; and cake thickness 0.4 in.

In order to confirm the particle size, the reagent adsorption and moisture content relationships, a number of dewatering tests were conducted on the West Virginia coal (0.044 m^2/g) and Pittsburgh coal (1.09 m^2/g) samples. Table 5.4 shows the test result obtained using Span 80 (dissolved 33.3% in diesel). The test results showed that the low surface area coal could be dewatered using less than 1 lb/ton reagent, and higher dosages did not significantly change the moisture contents. However, the high surface area Pittsburgh sample could not be dewatered even with a 3-lb/ton reagent addition since the surface coverage by the surfactant molecules could not be significant. As a result, it can be concluded that higher surface area coal needs more surfactant to make the particles more hydrophobic for the dewatering processes.

XPS Analysis: The experimental test results were conducted on the Pittsburgh and Middle Fork coal samples. Figure 5.5 shows wide-scan XPS spectra of the Pittsburgh coal sample. The

experimental results show that oxygen (533.2 eV), nitrogen (400.5 eV), carbon (285.0 eV), sulfate (196 eV), elemental sulfur (164.5 eV), aluminum (75.6 eV) compounds were mainly presented into the coal structure. The inorganic compounds might be due to the clay and sulfur content of the coal samples.

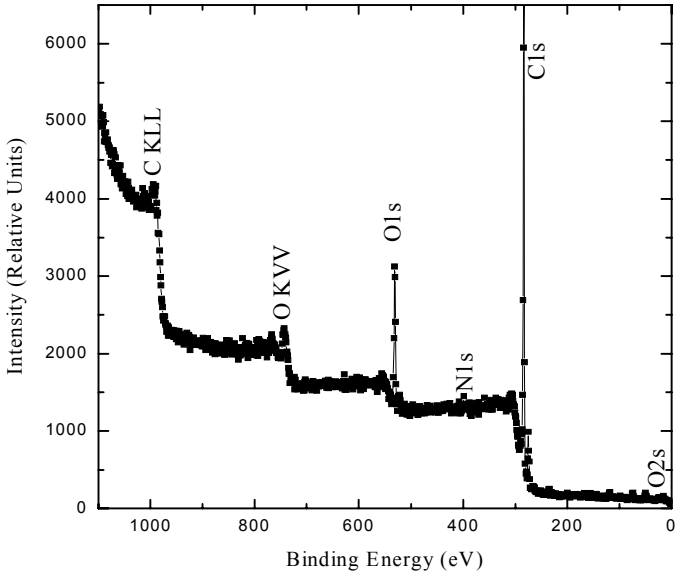

Figure 5.5 Schematic representation of XPS spectra (wide-scan) obtained on the Pittsburgh coal sample

Figure 5.6 shows a narrow-scan XPS spectrum of the Pittsburgh coal sample. The C (1s) photopeak was curve fitted for each compound. The spectra follow functionalized forms of carbon components at three peaks: C=O-C at 288.9 eV, C-O at 268.77 eV and C-C (or CH_2) at 285.09 eV binding energies. The single bonded C-O groups can be ether and hydroxyl groups contributing the most of the total oxygen contents in the coal sample. Also, carbonyls and carboxylates groups can make less contribution, which are consistent with the literature studies [104]. In addition to these, impurities in coal, e.g. clay, sulfate, carbonates, etc. may make the surface basic. van Oss and his colleagues reported that many solids had basic characteristics, which might be due to the O_2 atoms in the solid structure. Therefore, one can see that the coal may have basic charactrestics (γ_s^-) because of the oxygen atoms in the coal structure [17,95].

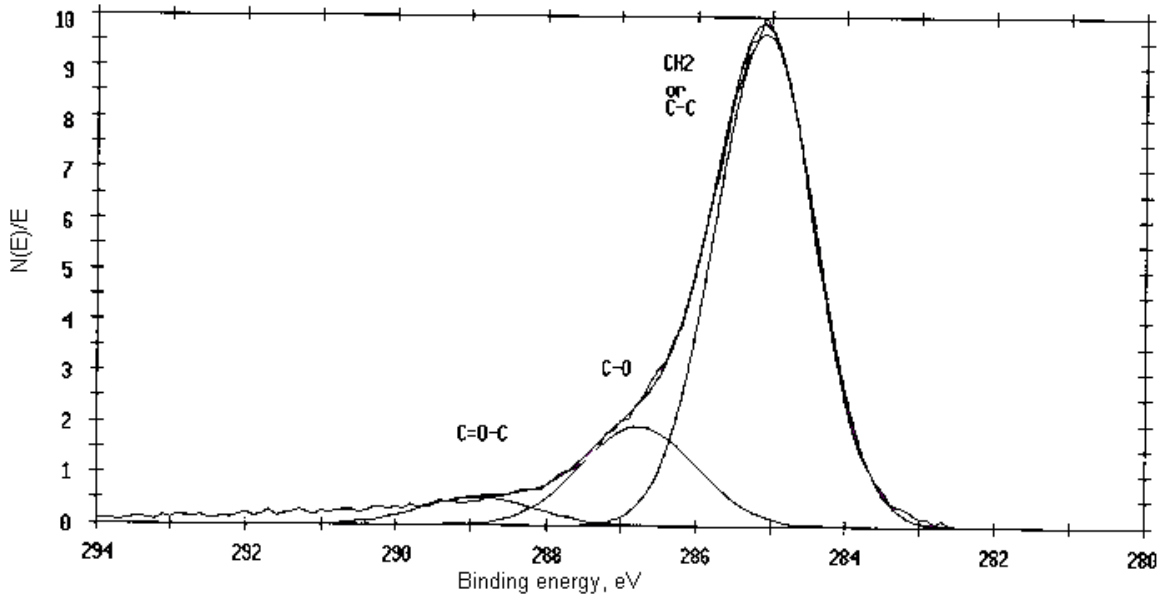

Figure 5.6 Narrow-scan XPS spectra of the carbon compounds on the Pittsburgh coal sample

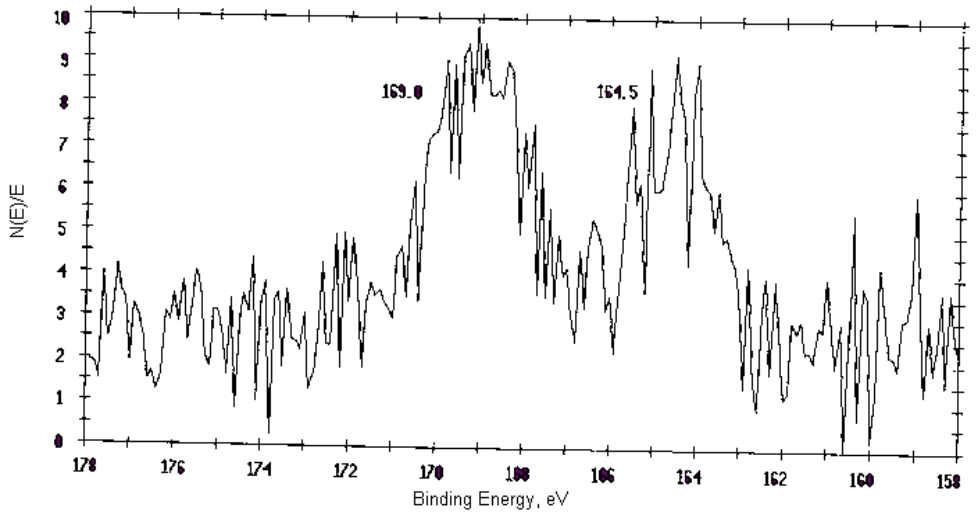

Figure 5.7 Narrow-scan XPS spectra of the sulfur compounds on the Pittsburgh coal sample

Figure 5.7 shows the narrow-scan XPS spectra of the sulfur compounds. The peaks of 169.0 eV and 164.5 eV binding energies corresponds to SO_4^{-2} and S^o. It is known that coal contains sulfur elements in its structure [4,47,48]. As a result, sulfur peaks of the coal sample indicate that the Pittsburgh coal has organic elemental sulfur and pyritic sulfur (pyrite and markacite). The later sulfurs are consistent with the conclusions of the LORLM image analysis conducted on the Pittsburgh coal sample.

Figure 5.8 shows the wide scan range spectra of the Middle Fork coal sample. The XPS spectra of the sample are the same as those obtained with the Pittsburgh coal sample. The results possess that the coal has mostly carbon, oxygen, nitrogen, silicon, aluminum and sulfur elements. However, the difference in the composition between two samples might be due to the organic and inorganic components of the Elkview coal sample or contamination during the sample preparation (sand papering).

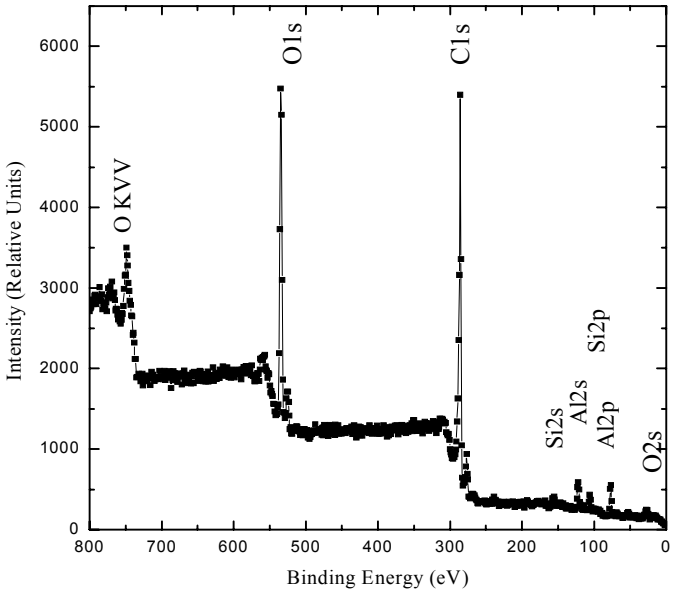

Figure 5.8 Schematic representation of XPS spectra (wide-scan) obtained on the Middle Fork coal sample

Figure 5.9 illustrates curve fitted carbon compounds obtained on the Middle Fork coal sample at narrow-scan size of XPS spectra. The shoulders in the vicinity of 285.0 eV indicate that the carbon species are in the form of C=O-C (288.7 eV), C-O (286.85 eV) and C-C or CH_2 (284.96 eV). These results are identical to those obtained with the Pittsburgh coal sample. This says that the coal surface may have basic compounds. In addition to the inorganic elements, it is also reported that ether groups, carbonyl groups and carboxyl groups of the coal sample exhibit basic characteristics and make the coal surface basic [17,47,48,94]. It has been mentioned in this study that the low HLB surfactant that had been used as the dewatering aids could only adsorb on the organic part of the surface and give higher moisture reductions.

The atomic concentrations of the Middle Fork and Pittsburgh coal samples are also given in Table 5.5. The test results show that both coal samples have similar elemental compositions.

However, the oxygen percentage of the Middle Fork coal sample is higher than that of the Pittsburgh coal. The reason can be contributions of the coal origin (e.g., ether, hydroxyl, carbonyls and carboxylates groups) or mineral matter in this particular Middle Fork coal.

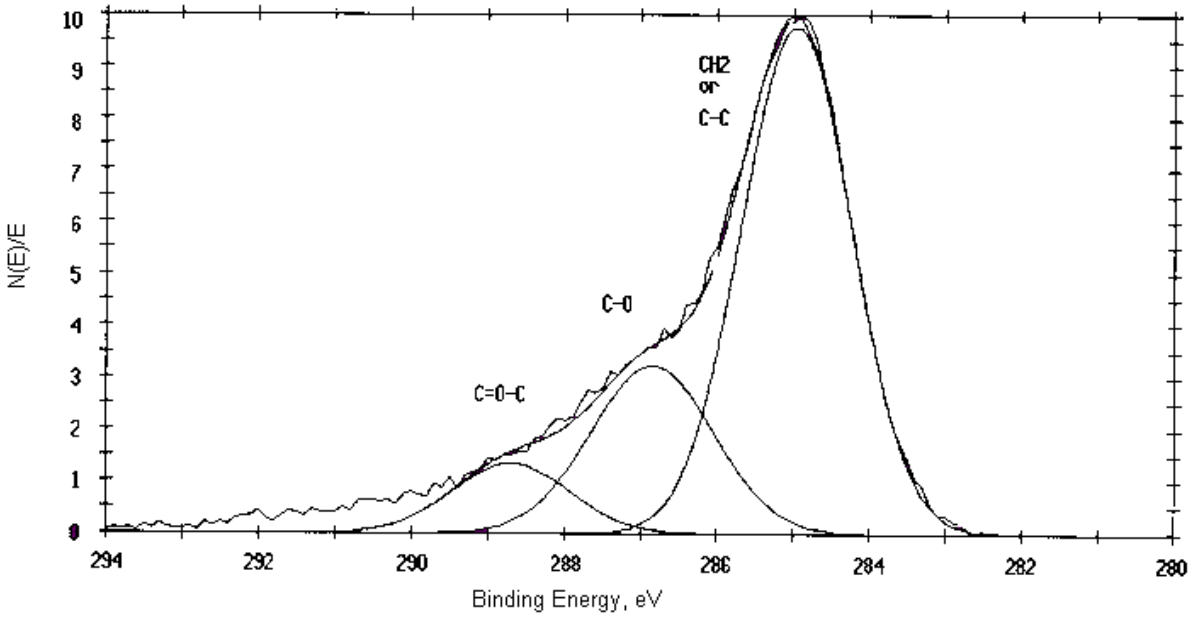

Figure 5.9 Curve fit C(1s) of the narrow-scan XPS spectra of the Middle Fork coal sample

Table 5.5 Atomic concentration of the coal samples obtained by XPS analyses

Elements	Atomic Concentration (%)	
	Middle Fork Coal	Pittsburgh Coal
C(1s)	65.14	84.35
O(1s)	25.13	11.81
N(1s)	0.69	1.41
S(2p)	0.48	0.63
Ca (2p)	0.09	<0.5[1]
Al(2p)	6.54	1.79
Fe(2p)	<0.5[1]	<0.5[1]
Si(2p)	1.93	<0.5[1]

[1] expected element percentages

Electrokinetic Studies: Figure 5.10 shows the ζ-potential data obtained using with and without aluminum sulfate ($Al_2(SO_4)_3.18H_2O$) on West Virginia and Pittsburgh coal samples as a function of pH. The experiments were conducted using nanopure water because tap water may have large amount of Cl^- ions and may change the surface charge of the particles. In the absence

of aluminum ions, the coal samples had positive ζ-potentials at lower pH, while they had negative values at the higher pHs (approximately 4). From the results, it is seen that the West Virginia and Pittsburgh coal samples gave 3.0 and 4.5 point of zero charges (PZC). In the presence of the metal ions, isoelectric points (i.e.p) values were sifted to natural pHs where the dewatering tests were usually performed in the plants. The reason may be attributed to the adsorption of Al^{3+} or $Al(OH)^{+}_{2}$ ions on the coal sample [16]. At pHs 6 and 7, the ζ-potentials became 0 or closer to 0 mV at which the finer particles could be coagulated due to the charge neutralization. This may provide an explanation of the electrolyte effects on the fine particles.

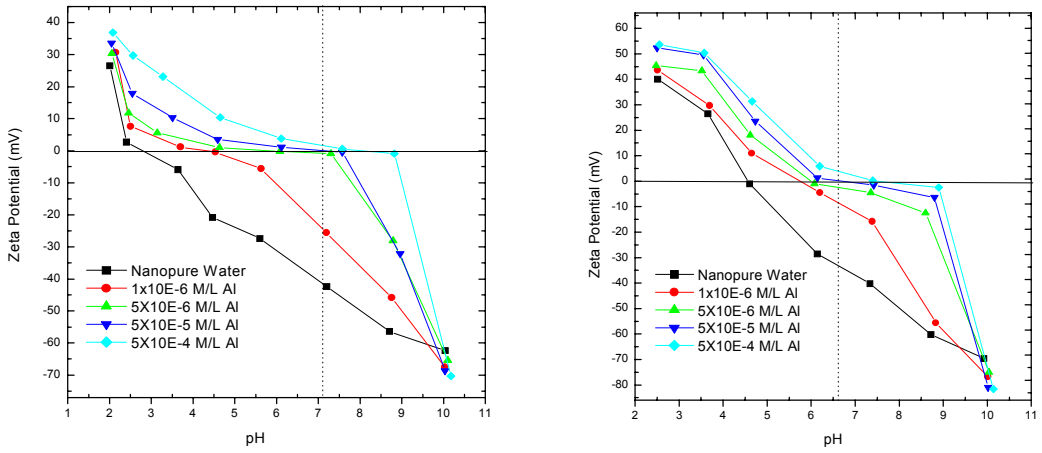

a b

Figure 5.10 Zeta potential of various untreated and treated a) West Virginia and b) Pittsburgh coal samples as a function of aluminum sulfate and pH

Honaker [69] and Xu [93] reported that coagulation of fine coal particles was practically impossible at higher ζ-potentials and possible at zero or closer to zero potentials. It is assumed that the coagulation of the particles can improve the moisture reduction and dewatering kinetics of the fine particles. In order to confirm this conclusion, a series of dewatering tests were conducted on the West Virginia and Pittsburgh coal sample (0.3 mm x 0) in the presence and absence of aluminum ions. In each experiment, the coal samples were conditioned with the electrolyte for 5 minutes and then introduced to the dewatering tests at a 25-inch Hg vacuum pressure, 2 minutes of drying cycle time and 0.4 inches cake thickness. The test results are given in Table 5.6.

The results indicated that the use of the electrolytes decreased the moisture contents of the fine coal samples. For example, a $5x10^{-5}$ M/L reagent could be required to achieve lower cake moisture. This might be due to the fact that trivalent Al^{3+} ions or its hydroxyl spices could go onto the fine coal particles and decrease the zeta potential (ζ = 0 mV) at neutral pHs. When the potential of the surface became zero by adding aluminum sulfate, these fine particles could be coagulated in the slurry and behaved as large particles in the filter cake. The larger particles could increase the capillary radius of the cake, and improved the dewatering performance of the fine particles (see Lablace equation) [16,69,93,117]. A similar result was obtained on the silica powder and the results are given with the AFM tests in the following sections.

Table 5.6 Effects of Using Aluminum Sulfate for the Filtration of West Virginia and Pittsburgh Coal Sample

Electrolyte Dosage	Moisture Content (% wt.)	
(M/L)	West Virginia Coal	Pittsburgh Coal
0	21.5	22.8
$1x10^{-6}$	20.3	22.0
$5x10^{-6}$	17.6	19.3
$5x10^{-5}$	17.4	19.2
$5x10^{-4}$	17.7	19.7
PH[1]	7.1	6.6

[1]pH was adjusted by adding diluted HCl and NaOH solution

5.3.2 Acid-Base Interactions on Solids and Liquids

Acid-base components may be needed to understand the mechanisms of the filtration, flotation, agglomeration, flocculation and coagulation processes. In these processes, the major concept is to eliminate the hydrophilicity and charge of the particle surfaces [17,63,69,93-103]. In this section, it will be shown how the acid-base components of solid and liquid (γ_{ij}^{AB}) can be determined and how they affect the moisture contents of the cake.

Coal samples, which are naturally hydrophobic materials, may show acidic and basic groups in its structure. It was determined that the ether groups, carbonyl groups and carboxyl groups of the sample exhibited basic behavior over the coal sample. In addition, the basicity of

the sample can be increased because of some impurities, such as sulfate, clay, shale, limestone, silica and iron oxide in the coal sample. The basicity of these minerals is due to the oxygen compounds of the particles [17]. Therefore, these minerals may adsorb hydroxyl ions in water, which makes the surface hydrophilic. Several investigations showed that coal and graphite samples were slightly basic or apolar materials depending on the coal ranks and gave a wide variety of hydrophobicity and hydrophilicity characteristics [17,43,71,93,94,97,100].

van Oss and his colleagues reported that a basic surface could need an acidic surfactant for a surface coverage if the surface of the solid consisted of hydrogen bonding in water [17,93-95]. In order to determine this phenomena, several solids and liquids were subjected to surface characterization tests to find the surface energies of the materials. Using the obtained data, one can determine the acid-base interaction between coal surface and surfactant molecules.

Surface Characterization of Coal Samples: Four different coal samples from Elkview, Middle Fork, Pittsburgh and Massey were subjected to surface characterization tests. Each coal sample was polished using appropriate methods explained above. The contact angle measurements were conducted using a sessile drop technique to measure advancing contact angle θ_a. For each sample, three known liquids, namely water, glycerol and mehtyleniodide given in Table 5.11 were used and then the average contact angle values were put into the Equation [13]. Three unknown equations were then solved to determine the surface components in the form of surface free energy. The contact angle measurements and the surface parameters of the coal samples are given in Tables 5.7 and 5.8, respectively.

Table 5.7 The values of the contact angles on the coal samples* using known Liquids

Liquids	Contact Angle (∓ 3°)			
	Pittsburgh Coal	Virginia Coal	Elkview Coal	West Virginia Coal
Water	46	49	45	44
Glycerol	40	42	37	38
Methyleniodide	19	20	22	18

The test results showed that water, glycerol and methyleniodide gave approximately 46°, 40° and 20° contact angle values on the polished coal samples, respectively. Likewise, it was calculated that the surface free energies of the samples were around the 55s mN/m. The results

indicated that the surfaces of the coal samples were mainly basic characteristics and acidic surface energy was only around 1 mN/m because of the formation of aliphatic, naphthenic and aromatic groups in the coal. The basicity of the coal sample came from ether, hydroxyl, carbonyls and carboxylates groups and mineral matters, which agree well with the XPS studies. It was also reported that if the surface was oxidized during the storage in air or water, the basicity of the sample could be increased [17,93-100].

Table 5.8 The surface tension components of different region coal samples

Surface Components	Coal Samples			
	Pittsburgh Coal	Virginia Coal	Elkview Coal	West Virginia Coal
γ_s^{LW}	46.18	45.90	45.31	46.44
γ_s^{+}	0.90	0.62	1.39	0.98
γ_s^{-}	24.81	27.93	23.73	25.91
γ_s^{AB}	9.45	8.32	11.49	10.08
γ_s	55.63	54.22	56.80	56.52

It is the assumption of the investigation that the low HLB surfactant can work on the slightly hydrophobic surfaces. These can be naturally hydrophobic or initially hydrophobized surfaces using flotation techniques. Therefore, the dewatering aids can only make hydrophobic parts more hydrophobic in dewatering. It is also assumed that there may not be interactions between the hydrophilic part and reagents. The obtained results are also consistence with these assumptions and literature studies [9,103-106].

Characterization of Low HLB Liquids: Several low HLB surfactants developed at Virginia Tech were used as dewatering aids on the fine coal and mineral particles. It was seen that some of the reagents worked better than the others on the particles. In order to understand this phenomenon, a series of reagent characterization tests were conducted on the smooth surfaces of teflon, mica and glass substrates. The surface components of the solids are given in Table 5.10. Due to the lower surface tensions (~25-27 mN/m) of the liquids (TDDP, ROE, Span 80 and SBO) dissolved 33.3% in diesel, the contact angle measurements of mica and glass were conducted in water to be able to receive significant contact angle values. The former substance, which is an apolar material, has a lower surface tension and it gives a significantly higher contact

angle values into air. Tables 5.9 gives the surface components of the liquids obtained using contact angle measurements.

Table 5.9 The surface tension* components of reagents used as dewatering aids

Surface Components	Dewatering Reagents				
	TDDP	ROE	Span 80	SBO	Diesel
γ_l^{LW}	25.00	26.71	26.01	26.57	26.1
γ_l^{+}	7.79	6.45	7.61	0.02	0.0
γ_l^{-}	0.16	0.06	0.10	5.41	0.0
γ_l^{AB}	2.24	1.19	1.69	0.53	0.0
γ_l	27.24	27.90	27.70	27.10	26.1

Table 5.10 The surface tension components of the known solids and liquids

Surface Components	Solids			Liquids		
	Teflon	Mica	Glass	Water	Glycerol	Methyleniodide
γ_l^{LW}	18.04	36.5	34.0	21.8	30.00	48.8
γ_l^{+}	0.00	0.2	1.0	25.5	3.92	0.0
γ_l^{-}	0.00	57.7	64.2	25.5	54.70	0.0
γ_l^{AB}	0.00	6.8	15.8	50.1	30.00	0.0
γ_l	18.04	43.3	49.8	72.8	64.00	48.8

The test results show that the contact angle values of the liquids varied, depending on the acid-base parameters of the substances. This might be the indication of the acid-base interactions of the liquids on the solid surfaces. According to the test results, it was determined that TDDP, ROE and Span 80 were slightly acidic, while SBO was merely basic and Diesel was nonpolar liquids. Even though the basic parts of the first three liquids are low levels, they should adsorb on the basic surfaces in water. XPS studies also confirm that the coal samples consist of ether, hydroxyl and carbonyls groups, which have oxygen compounds to support this conclusion. To be able to experimentally show this issue, a series of dewatering tests given in Table 5.11 were conducted on the Middle Fork dense medium coal samples (0.6 mm x 0) using a 2.5 inch diameter pressure filter at 100 kPa air pressure. The samples were crushed, ground, and floated, using 300-g/ton kerosene and 75-g/ton MIBC before the tests.

Table 5.11 The effects of acid-base interactions on dewatering of Middle Fork coal sample using different reagents at 100 kPa air pressure

Reagent Dosages (lb./ton)	Moisture Content (%)			
	TDDP	ROE	Span 80	SBO
0	24.7	24.7	24.7	24.7
1	17.3	18.5	16.1	19.4
2	14.4	16.0	13.8	17.9
3	12.8	14.3	12.4	16.6
5	11.7	13.9	12.0	15.9

The results proved that when the acidic reagents were used on the basic coal surface as dewatering aids, the moisture reduction of these reagents was higher than that of the basic reagent. For example, at 3 lb./ton reagent TDDP, ROE, Span 80 and SBO additions, the moisture contents of the cake were decreased from 24.7% to 12.8, 14.8, 12.4 and 16.4%, respectively. As seen, the basic reagent gave higher moisture contents. This observation offers an explanation that the acidic reagents may adsorb on the solid surface via both γ_l^{LW} and γ_l^{AB} interactions; nonetheless, the basic reagent may not have this interaction (only γ_l^{LW}). It was also pointed out that the structure of the SBO might be affecting the reagent adsorptions. As a result, the moisture differences between the acidic and basic reagents may be due to the acid-base interactions on the surfaces and the structure of the surfactants.

It is reported that there is a relationship between surface hydrophobicity, work of cohesion *Wc*, work of adhesion *Wa* and surface free energy *ΔG* of solids [14-18]. The work of cohesion occurs between the water molecules:

$$Wc = 2\gamma_{lv} \qquad [26]$$

The surface free energy of the solid is related to the work of adhesion between solid and liquid:

$$Wa = \gamma_{lv} + \gamma_{sv} - \gamma_{sl}, \quad \text{or}$$

$$Wa = -\Delta G = \gamma_{lv}(1+\cos\theta) \qquad [27]$$

where γ_{lv} is liquid-vapor, γ_{sv} is solid-vapor, γ_{sl} is solid-liquid surface tensions and θ is contact angle. As known, hydrophobicity of the solid becomes dominant when the work of adhesion is lower than that of the cohesion [18,74]:

$$Wa < Wc, \text{ or}$$

$$W_a^d + W_a^p < Wc \qquad [28]$$

at which W_a^d is apolar surface energy and W_a^p is polar surface energy. The last term is also associated with the acid-base interaction γ_s^{AB} in water. Adding surfactant to the slurry, Wc becomes larger than Wa to decrease this value. This also makes the surface more hydrophobic. Pazhianur and Yoon [63] have reported that the values of γ_s^{AB}, γ_s^- and γ_s^+ decreased with increasing the surface hydrophobicity (or contact angle). The decrease in γ_s^{AB} is due to the decrease in γ_s^- and γ_s^+ (see Equation [13]) in the presence of surfactant. As noted, the dewatering aids also increased the contact angel of the fine particles and gave higher moisture reduction. Therefore, one can conclude that adding the low HLB surfactants decrease the work of adhesion of the particles and make the surface more hydrophobic [74,94,118-130]. This may be the reason for the higher moisture reduction obtained on the fine particles dewatering.

5.3.3 Surface Coverage Studies

In these studies, palsed laser deposition (LPD), Langmuir-Blodgett (LB) and FTIR works were conducted on the samples to be able to determine properties of the surfactant formed on the sample surface. As known, the dewatering aids used in the present work cannot adsorb on the hydrophilic silica surface, but can adsorb on the hydrophobic carbon surface. Graphite is a naturally hydrophobic material and gives the higher contact angles. For this reason, both sides of the silica plates were coated by carbon to determine the surfactant molecules on the surface. In these tests, the carbon coating on the silica plates were conducted using PLD technique at 5.5×10^{-5} torr vacuum pressure and room temperature. The thickness of the carbon film on the silica plate, which is more than 80% diamond like carbon, was approximately 50 nm. Figure 5.11 shows the Digital Instrument Dimension 3000 AFM image analysis of the clean silica surface and carbon coated silica surface. The image analyses confirmed that the silica plate surface was well coated by carbon atoms. In addition, contact angle measurements using Sigma70 on the

coated surface gave higher contact angles (between 54° and 64°), while silica plate alone gave only 6°.

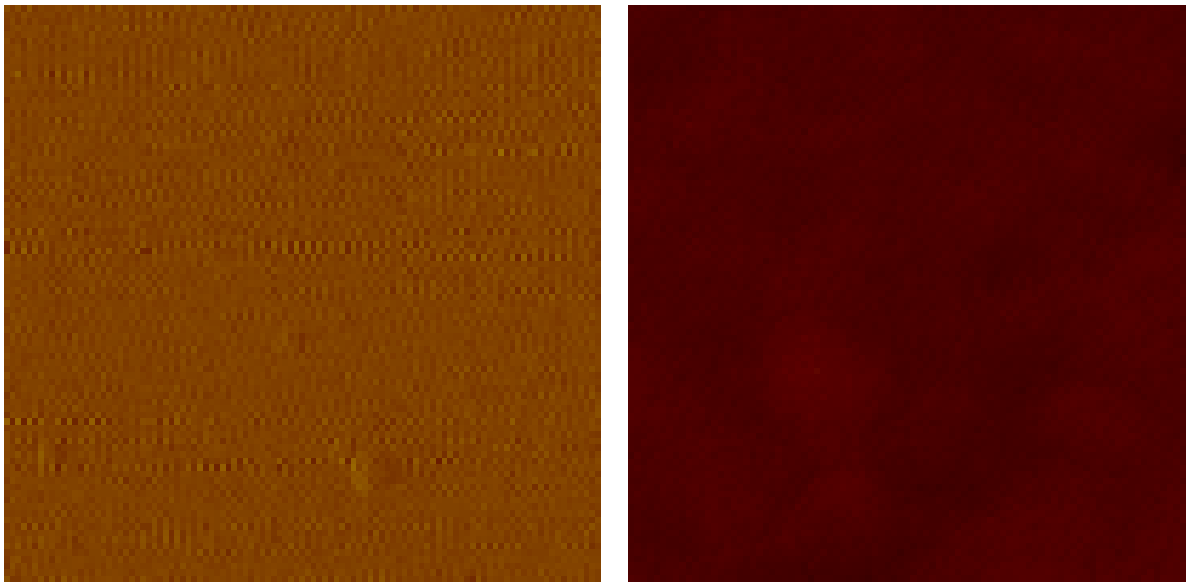

a) b)

Figure 5.11. Results of the AFM image analysis of a) clean silica surface and b) PLD carbon coated silica surface. Dimension is 100 x 100 nm, and height is 10 nm.

The carbon-coated plates were then coated by the LB film deposition method in the presence of dewatering aids. The LB tests using KVS-LB instruments on the carbon coated silica surface displayed that two collapsing behaviors of the reagent Span 80 (dissolved 33.3% in diesel) were seen at 18.6 mN/m and 40.8 mN/m film pressures. This may be attributed to the reagents compositions (Span 80/diesel = ½). Therefore, the surfactant coating with the LB technique was conducted at 18.6-mN/m film pressure. The LB results showed that there was no monolayer formation on the carbon surface, which may be due to the diesel molecules presented in the reagent. However, the same experiments illustrated that there was surface coverage by the surfactant molecules since the contact angle of the plate was increased from 64° to 78°.

To better understand this phenomenon, a series of FTIR analyses were carried out on the carbon surface coated by LB technique using Span 80. However, the results indicated that only CH_2 and charbonyl compounds of the reagent could be seen from the FTIR works. This may be due to the fact that an electron beam of the FTIR was adsorbed by the carbon surface and

significant molecular peaks could not be obtained for all the surfactant molecules. The data presented in this study are inconclusive regarding whether the dewatering surfactants have interactions (e.g., multi layers, oily droplets, lens shape between the particles, partially coating, etc.) in the interface, and this interaction can improve overall dewatering performance. Therefore, the question remains as to what interactions are responsible for the surface coverage of the dewatering aids. Further investigations into the bonding mechanism and their effects on the surface hydrophobicity changes are needed to be researched by using new techniques and approaches.

5.3.4 Surface Force Measurements

In the present work, electrolyte and surfactant effects on the surface forces of the materials were studied using an AFM. As known, the electrolytes cause coagulation by decreasing the surface charge of the colloidal particles, which is directly associated with the surface forces of those particles. It was reported that natural silica particles (negatively charged at pH>2) were not coagulated at any pHs due to the repulsive interaction (or hydration forces) in water [93]. However, it was also reported that silica particles could be coagulated in the presence of electrolytes [14-18,74], which have been sought for the dewatering process of this work.

Figure 5.12 shows a) $CaCl_2$ effects on the zeta potential of the silica particles as a function of pH and b) the surface forces measurements in nanopure water at pH 9.75 and 20 °C. The results of the electrokinetic experiments conducted on silica samples with and without electrolyte showed that the zeta potential of the particles decreased with increasing electrolyte concentration. At the lower $CaCl_2$ concentration, i.e.p. of the particles were around pHs 11 and 12; however, at $5x10^{-2}$ M/L concentration, it was shifted to 9.75, which is probably due to the adsorption of singly charged monovalent hydroxy-complexes (e.g., $CaOH^+$) on the silica surface. This result agrees well with the distribution diagrams of the calcium spices given in the references [16,68]. In addition, at the high reagent dosages, the surface charge of the particles was closer to zero where the coagulation is favorable. The similar zeta potential results were also obtained for the coal samples in the presence of the aluminum sulfate at natural pHs.

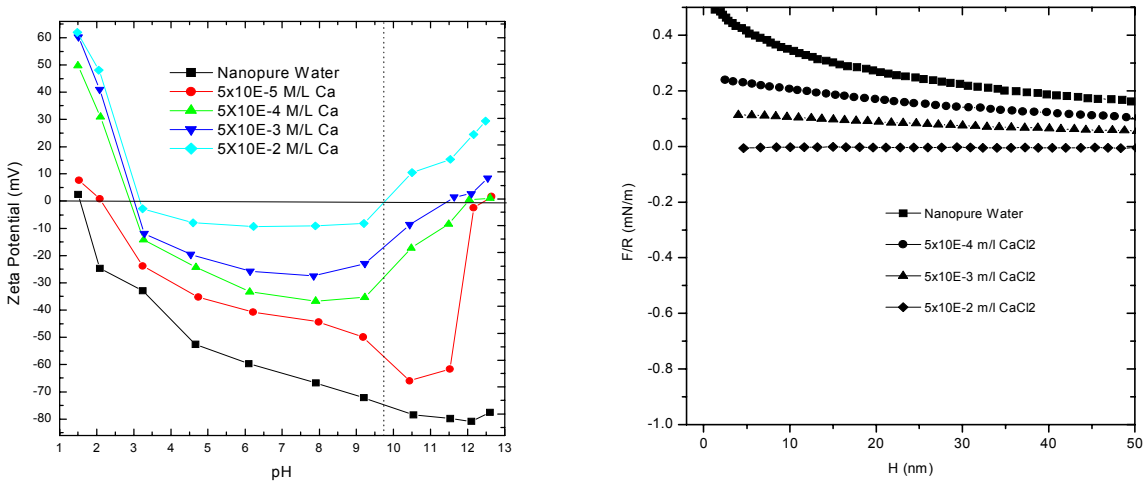

a) b)

Figure 1.12 a) $CaCl_2$ effects on the zeta potential of the silica particles as a function of pH, b) F/R vs H curves obtained between silica plate and glass sphere in the presence of $CaCl_2$ at pH 9.75. The dashed lines represent the classical DLVO theory, and the symbols represent the experimental results fitted for the force data

It is assumed that when the surface charge of the particles was decreased, the attractive forces (e.g., van der Waals) between the particles can be maximized, which is shown in Figure 1.12b. The first solid line represents the DLVO fit with Hamaker constant of silica **1** in water **3** $A_{131} = 8x10^{-21}$ J, $\Psi_1 = -60$ mV and $\kappa^{-1} = 42$ nm. As seen, the surface forces measured at H< 3 nm separation distance are attributed to the repulsion double layer forces (or hydration force) at pH 9.75. However, in the presence of divalent cation, the hydration force gradually decreases based on the electrolyte concentration and completely disappears at $5x10^{-2}$ M/L $CaCl_2$. This disappearance can be due to the fact that the calcium hydroxy species react with the negatively charged silica surface and make it neutralized. The electrokinetic studies also confirm this observation. Consequently, the surface hydrophobicity of the silica particles was enhanced significantly by the electrolyte additions, which should affect the dewatering of fine particles.

In order to determine the relationship between zeta potential, surface force and the dewatering of the fine particles, a series of dewatering tests were conducted on the fine silica powder using $CaCl_2$ and CaO in nanopure water at pH 9.75. The test results are given in Table 5.12. An important observation made in the present work was that the dewatering kinetic and

moisture reduction were higher with the divalent cations. At that pH, attractive force of the surface is also higher to decrease the hydration forces of the glass sphere and silica plate in water. It can be because of the fact that strongly hydrated water molecules on the silica surface are displaced by the singly charged calcium hydroxy species. For this reason, the dewatering of fine particles could be improved. The author also observed that at the higher electrolyte concentration, coagulation of the silica particles in a beaker was visually seen in a short time (in a few minutes).

Table 5.12 Dewatering test results on silica sample* using $CaCl_2$ and CaO at 25 inHg Vacuum Pressure and pH 9.75

Electrolyte Addition (M/L)	Moisture Content (% wt.)	
	$CaCl_2$	CaO
0.0	25.4	25.4
$5x10^{-5}$	24.8	24.7
$5x10^{-4}$	24.0	23.9
$5x10^{-3}$	20.6	20.8
$5x10^{-2}$	18.0	18.3

* 2.5 inch vacuum pressure filter used; sample prepared in nanopure water; particle size 0.038 mm x 0; 2 min. drying cycle time; cake thickness 0.4 in.

Surface force measurements between glass sphere and silica plate were also conducted in the presence of dodecylamin hydrochloride and dewatering reagents. In the amine tests, the force measurements given in Figure 5.13 were carried out at different dosages and pH 5.8. As can be seen, the hydrophobic force increases as a function of the amine dosages and reaches a maximum at $1x10^{-4}$ mole/lt. Since then, it was observed that there was no significant change on the particle hydrophobicity. Overall, the measured hydrophobic force can be an evidence of hydrophobic improvements of the dewatering reagents for the particles to be dewatered at higher contact angles. The results also agree well with the previous test results conducted on the silica surfaces to find out the mechanisms of the flotation and coagulation of the fine particles [61-69].

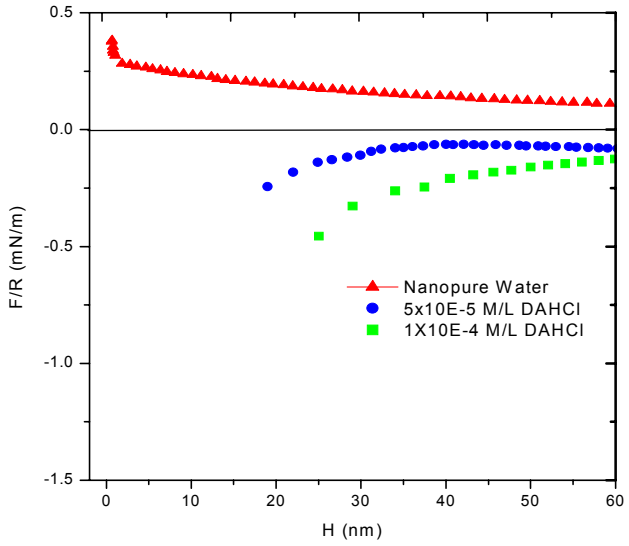

Figure 5.13 Results of the AFM force measuremnts conducted between the glass sphere and silica plates in the presence of the reagent DAHCl at pH 5.8. The solid lines represent the classical DLVO theory, and the symbols represent the experimental results fitted for the force data. A power law has been used for the hydrophobic curve fitting. K values are $5x10^{16}$ J and $8x10^{16}$ J, respectively.

In the dewatering aid experiments, tests were carried out in three steps. The first one was without chemical, the second was with a small amount of dodecylamine hydrochloride ($5x10^{-4}$ mole/lt.) to make the surface slightly hydrophobic and the third was additions of $2x10^{-5}$ and $5x10^{-5}$ M/L reagent Polymethylhydrosiloxane (PMHO) to obtain higher surface hydrophobicity. All tests were conducted at around 40 to 45 °C temperature due to the solubility improvements of the low HLB chemicals on the surfaces. The K values of the test were selected to fit the extended DLVO theory [65,67]. The results are shown in Figure 5.14. As seen, in the nanopure water the surfaces are completely hydrophilic and give repulsive forces. At $5x10^{-4}$ mole/lt DAHCl, the silica surfaces becomes weakly hydrophobic; however, in the presence of $2x10^{-5}$ and $5x10^{-5}$ mole/lt PMHO, the attractive force is significantly greater which may be attributed to the closed-pack monolayer formation on the surfaces. It was also measured that contact angles of the silica plate was ~97° where the maximum hydrophobic forces were reached in these tests. Thus, there is a good correlation between dewatering data and hydrophobic forces obtained using amine as a first hydrophobization and PMHO as a second hydrophobization aids.

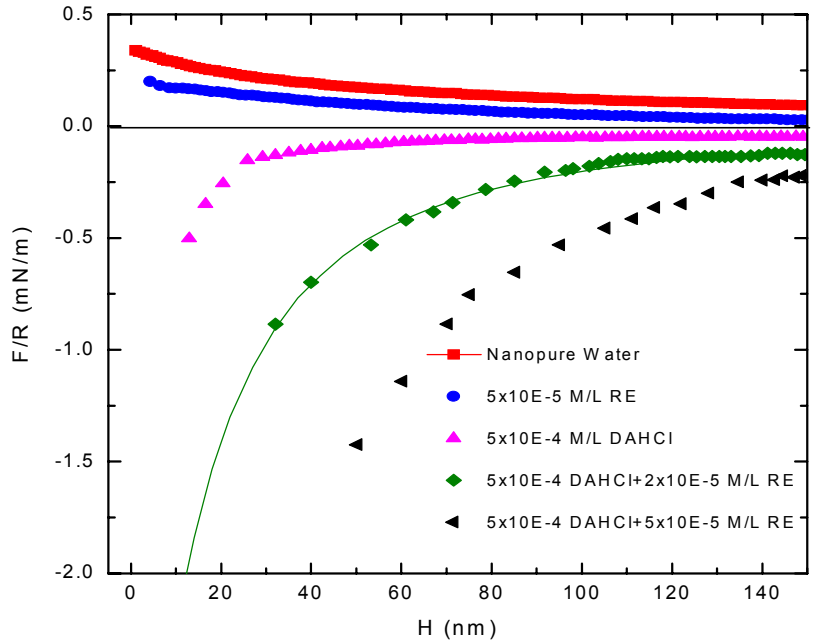

Figure 5.14 Results of the AFM force measurements conducted between the glass sphere and silica plates in the presence of the DAHCl and PMHO at pH 5.8 and ~40 °C. The solid lines represent the classical DLVO theory, and the symbols represent the experimental results fitted for the force data. A power law has been used for the hydrophobic curve fitting. K values are $5x10^{16}$ J, $5x10^{18}$ J and $2x10^{19}$ J respectively.

In addition to the PMHO, Span 80 dissolved in 20% butanol was also used for the force measurements following the same procedure of the former test. The result was shown in Figure 5.15. When the force measurements were carried out with only silica surfaces having approximately $\theta = 0°$, the measured force was repulsive because of the double layer interaction. At lower contact angles, the data was fitted to the DLVO theory with the Ψ_1 = -60 mV, $A_{131}=8x10^{-21}$ j and κ^{-1} = 42 nm. However, at higher contact angle actual jump distance was varied and the extended DLVO theory was used to fit the curves [63,65,67,68]. The data show more definitive evidence for existence of the hydrophobic force using second hydrophobization reagents, which has been modeled and used for these studies.

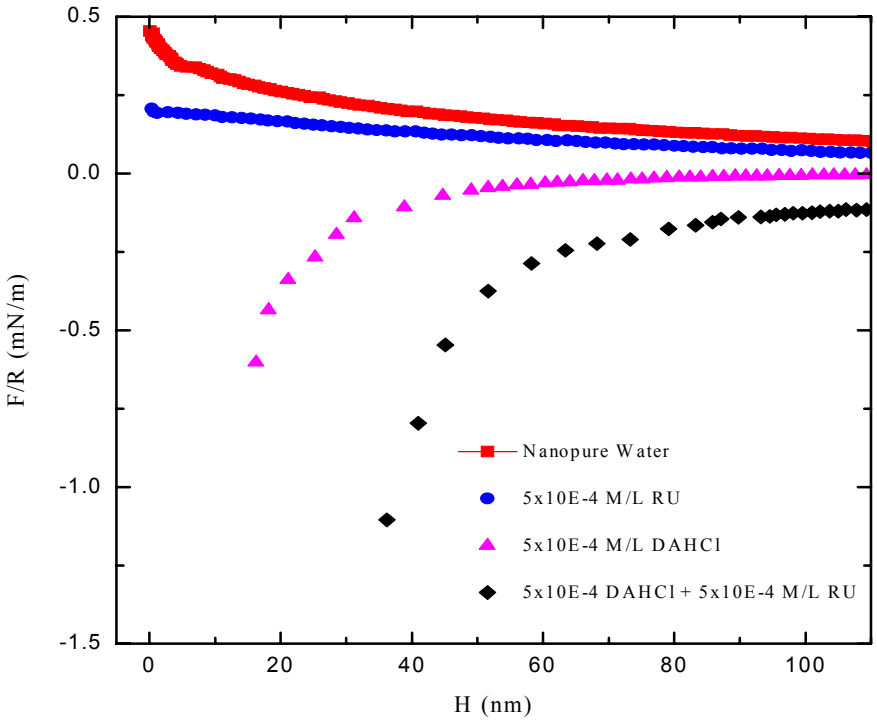

Figure 5.15 Results of the AFM force measuremnts conducted between the glass sphere and silica plates in the presence of the DAHCl and Span 80 (dissolved 20% in diesel) at pH 5.8 and ~40 °C. The solid lines represent the classical DLVO theory, and the symbols represent the experimental results fitted for the force data. A power law has been used for the hydrophobic curve fitting. K values are $8x10^{16}$ J and $1.25x10^{19}$ J, respectively.

Table 5.13 Dewatering test results on silica sample* using dodecylamine hydrochloride and dewatering aids at 25 in. Hg vacuum pressure and pH 5.8 and 40 °C

Reagent Addition (M/L)	Moisture Content (% wt.)		
	DAHCl	$5x10^{-5}$ DAHCl + PMHO	$5x10^{-5}$ DAHCl + Span 80
0.0	23.5	22.5	22.5
$5x10^{-5}$	22.5	15.3	14.5
$5x10^{-4}$	18.2	9.2	9.5
$5x10^{-3}$	17.0	8.1	7.7

* 2.5 inch vacuum pressure filter used; sample prepared in nanopure water; particle size 0.038 mm x 0; 2 min. drying cycle time; cake thickness 0.4 in.

In order to demonstrate the relationship between the hydrophobicity and dewatering, a series of dewatering tests were conducted on a 0.038 mm x 0 size silica powder at pH 5.8 and 40 °C. A 2.5-inch diameter Buchner funnel was used at a 25 in. Hg vacuum pressure, 2 min drying cycle time, and 0.4 inches cake thickness. The test results obtained using DAHCl, PMHO and Span 80 (20% in butanol) are given in Table 5.13. In the absence of the dewatering aid, the cake moisture was 23.5%; however, if DAHCl and dewatering aids are used together, the moisture was reduced to around 8%. As a result, the improved dewatering brought by the low HLB surfactants is most likely due to the hydrophobic enhancement (or contact angle improvements). These results agree well with the results of the dewatering tests given in the Chapters 2, 3 and 4, which may be due to the same reason.

5.3.5 Dewatering Kinetics Tests

The dewatering kinetic tests were conducted on Pittsburgh, Elkview and West Virginia DMC samples in the presence and absence of dewatering aids. In the first test, the Pittsburgh coal samples were crushed and ground to -1 mm and then floated using 1 lb./ton kerosene and 100 g/ton MIBC before the experiments. The test measurements were carried out on the slurry sample consisting of a 16-18% solid content with and without Span 80 (dissolved 33.3% in diesel) additions.

Figure 5.16 obtained using Equation [17] shows the kinetic test results of the Pittsburgh coal sample plotted as cake formation time/filtrate volume (t/V) versus filtrate volume (V). From the results, two striking observations were found on the dewatering of the fine particles when a designated amount of chemical was added to the slurry. *One*, the reagent addition caused the lines to differ in slope, which suggested that the cake parameters were changed. For example, the slope of the base line tests is higher than that of the dewatering aid lines. Also, the slope of the line gradually decreased when the magnitude of the reagent was increased. At a 5-lb./ton reagent Span 80 addition, slope of the line is almost parallel to the x-axis due to the higher dewatering kinetics of the present coal sample. *Two*, increasing the reagent dosage decreased interception of the lines, which means that medium resistance, was also reduced. Table 5.14 shows the change in cake parameters with and without Span 80. The results illustrated in Table 5.14 gives 12 important trends on the cake parameters that will be discussed in this section:

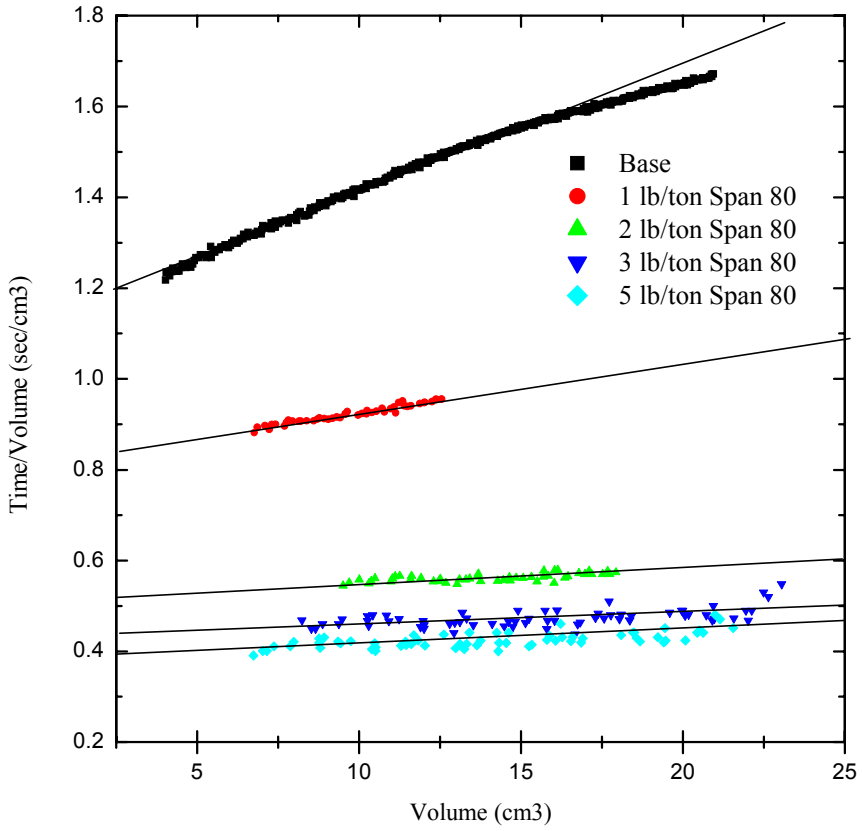

Figure 5.16 Effects of reagent Span 80 addition on the cake parameters of the coal sample at 60 kPa air pressure

Contact Angle: Contact angle measurements were conducted on the Pittsburgh DMS coal samples using Sigma70 device. Small chunks of the coal samples (rectangular 10x20x2 mm) were polished as explained and put into the screened slurry sample to condition with the chemicals [4,9,42,43,47,48]. For each region coal, seven measurements were carried out on different samples. The average values of the tests were then taken to be able to eliminate experimental errors. It was expected that the values of the contact angle were improved by increasing the amount of the reagent. Recognizing that increases in the hydrophobicity of the coal particle can be due to the surface coverage by the surfactant molecules. At a 5 lb./ton reagent, the contact angle increased from 21 to 88°. According to the Laplace equation, the pressure of the capillary water should be zero if the contact angle is 90°. This means that the water in capillary can be spontaneously removed without applying air/vacuum pressure. More

clearly, the water molecules under this condition cannot wet the particles [2,17,19,41,42,73]. Thus, the contact angle obtained using 5 lb/ton Span 80 would decrease a great deal of capillary pressure in the cake. In all of the dewatering tests, it was observed that, depending on the particle size (surface area) and the other dewatering conditions, applied pressures on the cake were significantly decreased due to the hydrophobicity improvements of the particles.

Table 5.14 Effect of reagent dosages on the cake parameters of Pittsburgh coal sample using Span 80 (dissolved 33.3% in diesel) at 60 kPa air pressure

Cake Parameters of Coal Sample	Reagent Span 80 Dosages				
	0 LB/ton	1 lb./ton	2 lb./ton	3 lb./ton	5 lb./ton
Contact Angle (°)	21	59	72	83	88
Filtrate Surface Tension (N/m)	0.072	0.068	0.063	0.060	0.056
Cake Resistance ($x10^{10}$, m/kg)	13.1	3.67	1.12	0.61	0.51
Medium Resistance ($x10^{9}$,m/kg)	4.03	2.80	1.70	1.47	1.33
Cake Permeability ($x10^{-14}$,m^2)	0.96	3.43	11.21	20.58	24.63
Kozeny Mean Diameter (μm)	2.7	5.1	9.3	12.5	13.7
Breakthrough Pressure (kPa)	29.3	8.2	2.5	0.8	0.2
Cake Formation Time (sec)	44	21	15	13	12
Measured Pressure (kPa)	60	45	40	35	35
Cake Thickness (in.)	0.56	0.58	0.60	0.61	0.61
Product Yield (%)	97.4	98.3	98.8	99.4	99.6
Moisture Content (%)	27.6	17.7	14.4	13.0	12.2

*2.5 in diameter air pressure filter connected to computer used; sessile drop technique used for contact angle measurements; Sigma 70 used for filtrate surface tension; size of sample 1 mm x 0; cake thickness 0.6 in.; cake porosity 0.41; breakthrough pressure constant α is 0.83; two minutes drying cycle time; DMC sample crushed, ground and floated using 1 lb./ton kerosene and 100 g/ton MIBC.

Yoon et al reported that the hydrophobic forces increased in the presence of surfactants onto the appropriate solid surface to be able to explain the mechanisms of flotation and coagulation processes of the fine particles [2,9,41,42,61-69,75]. The dewatering of the fine particles has not been studied well by varying the cake parameters; there are no significant data to compare these results to other published data. However, there are several base tests (no contact angle change, etc.) conducted on the cake dewatering by varying pressure, particle size and mineral types. These results are in consistent with the base tests carried out in these works [41,76-87]

Filtrate Surface Tension: In these tests, filtrate samples were taken at the end of the drying cycle time, and then the surface tension of the liquid was measured using a ring method of

a Sigma70 device. In the absence of the dewatering aid, the surface tension of the filtrate was 72 mN/m, which was very close to a pure water contact angle. As the reagent concentration was increased, the surface tension of the liquid was decreased to lower levels. With a 5-lb./ton-reagent addition, the surface tension of the liquid was dropped to 56 mN/m. Note that the surface tension of the reagent Span 80 is around 27 mN/m. Thus, it may be concluded that most of the reagent adsorbed on the coal surface for the contact angle improvements.

According to the Laplace equation, both surface tension and the contact angle can be responsible to enhance the dewatering of the fine coal samples, which is the objective of the present work. The literature studies showed that the surface tension of liquid was the major parameters in lowering the cake resistance and moisture contents of the fine particles [2,28,29,39-42,81,87-92]. Veal et al. reported that when the surface tension of liquid was decreased from 72 to 20 mN/m, moisture content was also decreased from approximately 25 to 22% [39,40,90]. However, the present study showed that the contact angle was the major parameter to achieve a low moisture content of the cake.

Cake Resistance: The cake resistance tests were performed on the fine clean coal sample (1 mm x 0) at 60 kPa-air pressure. A pressure filter in which a fine size filter cloth was placed as a filter media was used in the tests. During the dewatering period, filtrate was simultaneously collected into the graduated cylindrical tube including a pressure transducer connected to a PC. First of all, a plot of the volume vs. time was drawn on the screen of the computer, and then the data were converted into t/V vs. V to be able to find the slope and intercept of the lines. The test results are given in Figure 5.16. The obtained slope value was equated to the Equation [17] in order to find the specific cake resistance of the cake. The following parameters were accepted as constant values for all the tests:

- Cake thickness (L): 0.6 inches (0.153 m)
- Coal density (ρ_c): 1350 kg/m^3
- Filtrate density (ρ_f): 1000 kg/m^3
- Filtrate viscosity (μ): 0.001 Pa s.
- Cake porosity (ε): 0.41
- Filter surface area (A): 0.02 m^2
- Solid weight/filtrate volume (w): 291 kg/m^3
- Breakthrough Pressure constant (α): 0.83

The test results showed that the specific cake resistance of the base line is 13.1 x 10^{10} m/kg, which is identical to Veal et al results [39,40]. However, when a 1 lb./ton reagent Span 80 was added to the slurry, the specific cake resistance of the same sample became 3.67x 10^{10} m/kg. At a 5 lb./ton dosage, it was further reduced to 0.51x10^{10} m/kg, which corresponds to approximately 26 times lower cake resistance. As a result, it can be concluded that in the presence of the surfactant there is no need to use higher pressures to remove the water from the cake. It also saves a great deal of energy on the filter machines.

As known, the surfactant destabilizes (or liberates) the water molecules adhering on the surface of the coal particles by increasing the particle hydrophobicity at higher contact angles. In contrast, it does not play a role in transporting the liberated water through the filter cake due to the complexity of the cake structure. This transportation problem becomes more serious since the cake thickness is increased up to 1 inch. It was suggested in the present work that the filter cake could be subjected to a mechanical vibration to solve the existing problem.

Filter Medium Resistance: It is assumed that the filter medium resistance is always constant. However, the experimental results (see Figure 5.16 and Table 5.14) exhibited that the filter medium resistance was lowered depending on the reagent dosages. Although this odd finding is not clearly understood in the presence of reagents, it was assumed that there could be a hydrophobic coagulation between the fine coal particles. Therefore, the fine particles that can block the filter pores and increase the filter medium resistance can coagulate each other and remain as a larger particle in the cake. This may cause in decrease the filter medium resistance. In fact, it was also observed from the tests that when the reagent was added to the slurry, watercolor of the filtrate was clearer (less finer particles in the effluent) than watercolor of the base tests (more finer particles). This may be a reason of the hydrophobic coagulation of the ultrafine particles to decrease the filter medium resistance.

Cake Permeability: Permeability of the cake, which is obtained, using Equation [18], is strongly dependent on the specific cake resistance and the porosity of the sample. As shown, the base case of the permeability is 0.96x10^{-14} m^2; however, when a 2 lb./ton reagent Span 80 was added to the suspension, the cake permeability became 11.21 x10^{-14} m^2. At a 5 lb./ton-reagent addition, this value went up to 24.63x10^{-14} m^2, which gives 26 times more permeable cake. The reason is that in the presence of the reagent, the surface tension of liquid is reduced, the contact angle (or hydrophobicity) of the solids is improved and moisture in the capillary is decreased

(empty capillary tubes). Thus, these parameters cause the lower specific cake resistance and higher cake permeability for the fine samples. Similar explanations on the base case were given in the literature [5,8,13,24,27-29,37-42,87].

Kozeny Mean Diameter (KMD): The KMD is an average pore value for a whole cake, which is based on the cake permeability and cake porosity [5,8,39-42]. According to the Equation [20], the KMD value is sharply increased since the permeability and porosity of the cake is increased. The experimental results showed that in the absence of the reagent, the average pore diameter of the cake was 2.7 μm. Under the same conditions, if a 2 and 5 lb./ton reagent Span 80 were added to the pulp, this value increased up to 9.3 μm and 13.7 μm. This indicates that in the presence of the reagent, the fine particles behave as larger particles and give larger voids (capillary diameter) in the cake. This is desired conclusion for the fine particle dewatering of the present work.

Breakthrough Pressure: This pressure which is also called threshold pressure (see Equation [21]) is required a minimum pressure to remove the capillary water in the cake. Carlenton et al [41] determined that the pressure value is mainly dependent on the distribution of the pore size, contact angle, particle diameter, and liquid surface tension. In general, the higher the cake resistance, the lower the cake permeability, and the higher the threshold pressure occurs [5,28-30,39-42].

The experimental studies showed that the base line breakthrough pressure was 29.3 kPa; in contrast, when a 1 lb./ton reagent of Span 80 was added into the slurry, it appeared to be 8.2 kPa. A more interesting result was obtained with a 5 lb./ton-reagent addition where the contact angle was 88°. At this dosage, there was no need to apply more pressure to remove the capillary water since the breakthrough pressure had already been 0.2 kPa. The values obtained in this study proved the expected and the reported results [28-32,39-41,77,87]. Overall, the dewatering results can be satisfactory to use the low HLB surfactant as dewatering aids in the plant conditions.

Cake Formation Time: This time is the dewatering period ended when a bulk of the water was passed through the filter cake. At the end of this period, the drying cycle time starts for a couple of minutes, depending on the particle size, mineral types and the types of dewatering machines [5,8,13,87]. Several experiments were conducted on the fine coal samples to determine the cake formation times. The test results confirmed that in the presence of the reagents, the cake

formation time was substantially decreased. For example, cake formation time of 0 lb./ton and 5 lb./ton reagents were 44 sec and 12 sec. Thus, the cake formation time of the reagent test was approximately four times lower than that of the base test. This indicates that the change in the contact angle, surface tension, fine particle coagulation and the other cake parameters strongly affect the cake formation time.

Measured Pressure: When a designated amount of reagent was added to the suspension, all coal particles became more hydrophobic due to the surface coverage of the particles by the surfactant molecules. According to this explanation, the filter cake became more permeable where the cake resistance had minimum levels; as a result, the measured pressure would decrease based on the cake parameters. For instance, the test results given in Table 5.14 showed that the pressure was reduced from 60 kPa to 35 kPa with the addition of a 5 lb/ton reagent Span 80.

Cake Thickness: It is known that if the hydrophobicity of the particles is enhanced using surfactants, a hydrophobic coagulation occurs and causes particle enlargement [5.8,13,69,77, 87,93]. Therefore, it is expected that at a higher contact angle, the cake thickness should be increased. From the experimental result, in the presence of the reagent, a 5 to 15% cake thickness improvement was achieved on the coal sample as shown in Table 5.14. However, this thickness is not as high as with polymeric flocculation, which may be attributed to the fact that the flocculation effect is higher than the hydrophobic coagulation effect on the cake thickness [5,52].

Product Yield: Currently used industrial filters lose the very fine particles at the beginning of the suction or air pressure period, and it is worse for the screen bowel centrifuge filters [5,8,13,77]. However, test results from the research showed that if the reagent was introduced to the sample to be dewatered, the filter gave a 2% higher product yield as compared to the base line. This improvement in the product yield may be due to the hydrophobic coagulation of the fine/ultrafine particles at higher contact angle values.

Moisture Content: The main objective of using a low HLB surfactant is to increase the moisture reduction of the filter cake before further drying in thermal units. It is assumed that this reduction can be the improvements of the contact angle (or hydrophobicity). Shown in Table 5.14 are the equilibrium contact angles of the Pittsburgh coal samples treated under different reagent conditions. Without the reagent addition, the coal sample gave a contact angle of 21° giving rise to a relatively high capillary pressure, and hence, a high cake moisture. In the presence of the Span 80, the contact angle was gradually increased up to 88°. Therefore, this

should reduce the cake and filter media resistances, breakthrough pressure, cake formation time and wettability, and increase the particle diameter, permeability, product yield and moisture reduction in the filter cake. In the base case, it was observed that the product moisture was 27.6% at 60 kPa air pressure; meanwhile, when a 5-lb./ton reagent was added to the same slurry, it was reduced to 12.2% with 56% moisture reduction. Consequently, it is clear that this product does not need as much energy as the base case in the thermal dryers.

In addition to the Pittsburgh coal samples, similar tests were conducted on several fine coal samples. Table 5.15 shows the results of the pressure filter tests conducted on the Elkview coal samples using TDDP (dissolved 33.3% in diesel oil) as a dewatering aid. The coal sample was a dense medium product, which was pulverized, ball-mill ground, and screened at 0.3 mm. The screen underflow (-0.3 mm) was floated using 1 lb./ton kerosene and 100 g/ton MIBC before the tests. The filtration tests were conducted using 2.5 inches diameter pressure filter at 120 kPa-air pressure and 0.6 in. The other experimental producer and set-up were in the same manner of the first kinetic test.

Table 5.15 Effect of reagent dosages on the cake parameters of Elkview coal sample using low HLB TDDP (dissolved 33.3% in diesel) at 120 kPa air pressure

Cake Parameters of Coal Sample	Reagent TDDP Dosages				
	0 lb./ton	1 lb./ton	2 lb./ton	3 lb./ton	5 lb./ton
Contact Angle (°)	34	67	79	84	91
Filtrate Surface Tension (N/m)	0.072	0.067	0.061	0.059	0.055
Cake Resistance ($x10^{10}$, m/kg)	25.93	14.01	9.75	5.41	3.25
Medium Resistance ($x10^{9}$,m/kg)	7.21	5.21	3.93	3.01	2.67
Cake Permeability ($x10^{-14}$,m^2)	5.02	9.41	13.33	24.04	40.00
Kozeny Mean Diameter (μm)	1.75	2.41	2.86	3.84	4.95
Breakthrough Pressure (kPa)	37.01	11.95	4.48	1.77	-0.23
Cake Formation Time (sec)	48	30	20	15	13
Measured Pressure (kPa)	120	100	90	80	75
Cake Thickness (in.)	0.53	0.56	0.58	0.59	0.60
Product Yield (%)	97.2	97.9	98.6	98.9	99.4
Moisture Content (%)	27.2	20.0	15.1	12.9	11.7

*2.5 in diameter air pressure filter connected to computer used; sessile drop technique used for contact angle measurements; Sigma 70 used for filtrate surface tension; size of sample 0.3 mm x 0; cake thickness 0.6 in.; cake porosity 0.43; breakthrough pressure constant α is 0.83; two minutes drying cycle time; DMC sample crushed, ground and floated using 1 lb./ton kerosene and 100 g/ton MIBC.

The test results showed that contact angles of the Elkview coal sample increased based on the reagent concentrations. Without the addition of the reagent, the contact angle of the sample is 34°. With 1, 2, 3 and 5 lb./ton reagent additions, the contact angles became 67°, 79°, 84° and 91°, respectively, which means that hydrophobicity of the particles could be gradually improved on the surface of the particles. It was expected that such a large increase in the contact angle could be responsible for the substantial change in the cake parameters. As seen in Table 5.15, in the presence of 5 lb./ton reagents, the specific resistance of the cake was reduced 8 times, and hence, permeability was also enhanced in the same magnitude.

In addition the cake resistance, medium resistance, breakthrough pressure, cake formation time and measured pressure were substantially decreased, while the Kozeny mean diameter, cake thickness and product yields were also increased in the presence of the reagent additions. Finally, the moisture content of the sample was decreased from 27.2% to 11.7% with a 5 lb./ton reagent. All dewatering trends of these test results are also identical to the first tests conducted on the Pittsburgh coal sample.

Another set of pressure filter tests was conducted on the Massey-West Virginia coal sample using the reagent ROE (dissolved 33.3% in diesel), which is a modification of lard oil. The run-of-mine (ROM) coal sample was crushed, ground and screened to –0.6 mm, and floated with 1 lb/ton kerosene and 100 g/ton MIBC. The flotation product was subjected for filtration tests at 80 kPa-air pressure, 2 min. drying cycle time and 0.5 inch cake thickness. The experimental producers and set-up were the same as with the previous experiments. The test results are given in Table 5.16. As shown, the reagent ROE also increased the contact angle (or hydrophobicity) of the coal sample. When a 3 lb/ton reagent ROE was added to the slurry, the contact angle of the sample was enhanced from 35° to 87°, which corresponds a significant amount of hydrophobicity improvement on the coal particles. Therefore, increasing contact angle varied all the cake parameters to be able to receive lower moisture content from the cake. At a 3 lb./ton ROE, the moisture content of the cake was reduced from 26.2% to 14.2%, which are the similar to those obtained on the former tests. As a result, it can be concluded that the low HLB nonionic surfactants used in this investigation give remarkable moisture reductions and dewatering kinetics on the fine coal particles.

According to the Laplace Equation, the contact angle, surface tension and capillary radii are the main parameters for the higher moisture reduction. However, it is seen that even at higher

contact angles, there still exists moisture in the cake. This may be because of the fact that the capillary tubes of the filter cake can be more complex (vertical and horizontal tubes together) than the capillary tubes used for the Laplace equation (only vertical tubes). To better understand the cake structure, more detailed studies should be performed on the fine particles dewatering.

Table 5.16 Effect of reagent dosages on the cake parameters of West Virginia coal sample using Reagent ROE (dissolved 33.3% in diesel) at 80 kPa air pressure

Cake Parameters of Coal Sample	Reagent ROE Dosages		
	0 lb./ton	1 lb./ton	3 lb./ton
Contact Angle (°)	35	64	87
Filtrate Surface Tension (N/m)	0.071	0.064	0.058
Cake Resistance ($x10^{10}$, m/kg)	9.57	3.56	1.78
Medium Resistance ($x10^{9}$,m/kg)	4.69	2.71	1.69
Cake Permeability ($x10^{-14}$,m^2)	1.34	3.59	7.20
Kozeny Mean Diameter (μm)	2.99	4.95	7.01
Breakthrough Pressure (kPa)	22.3	6.50	0.49
Cake Formation Time (sec)	46	24	15
Measured Pressure (kPa)	80	65	55
Cake Thickness (in.)	0.48	0.52	0.54
Product Yield (%)	97.8	98.7	99.4
Moisture Content (%)	26.2	18.5	14.2

*2.5 in diameter air pressure filter connected to computer used; sessile drop technique used for contact angle measurements; Sigma 70 used for filtrate surface tension; size of sample 0.6 mm x 0; cake porosity 0.42; breakthrough pressure constant α is 0.83; two minutes drying cycle time; ROM sample crushed, ground and floated using 1 lb./ton kerosene and 100 g/ton MIBC.

5.4 SUMMARY AND CONCLUSIONS

Several coal samples from Pittsburgh, Elkview-Canada, Middle Fork-Virginia and Massey-West Virginia were subjected to surface characterization and dewatering kinetic tests. In the characterization work, the coal samples were prepared and used for the image, surface area, zeta potential, and elemental composition analyses. Also, the coal samples were used to determine the contact angle and acid-base components.

Surfaces of the polished Pittsburgh and Elkview coal samples were imaged using the LORLM technique. The test results showed that the coal surfaces consisted mainly of different coal macerals, sulfide and clay minerals. A more striking observation was seen on the Pittsburgh coal sample; this coal contained both pyrite and markacite. As known, the markacite has a high affinity to oxidation in water and it makes the coal surface more hydrophilic, which is not desrable in the chemical dewatering process.

The BET surface area tests were conducted on the fine Pittsburgh (0.1 mm x 0) and West Virginia (1 mm x 0) coal samples. The results showed that the West Virginia coal sample had a lower surface area than the Pittsburgh coal due to the larger size of the previous sample. Note that the higher surface area consumes larger volume of surfactant to make the particles more hydrophobic for the dewatering processes. The dewatering tests were also consistent with those conclusions.

XPS spectra of the Pittsburgh and Elkview coal sample showed that the coal surface consisted mainly of carbon, oxygen, nitrogen, sulfate, elemental sulfur, silicon and aluminum compounds. The inorganic compounds are due to the impurities (silicate, carbonate, sulfur, etc.) of the coal samples. However, the organic compounds presents the functionalized forms of carbon components, such as C=O-C, C-O and C-C (or CH_2). The C-O groups can be ether and hydroxyl groups contributing the most of the total oxygen contents in the coal sample. In addition, carbonyls and carboxylates groups can also contribute lesser effects on the basicity of the coal. Overall, one can see that the coal can have basic characteristic (γ_s^-) because of the oxygen atoms in its structure.

The electrokinetics studies conducted on the West Virginia and Pittsburgh coal sample indicated that the use of the electrolytes reduced the moisture contents of the filter cake. This may be attributed to the fact that trivalent Al^{3+} ions or its hydroxyl spices could go onto the fine coal particles and decrease the zeta potential of the particles (ζ = 0 mV) at neutral pHs. At zero or closer zero potentials, the fine particles could be coagulated in the suspension and settled as large particles on the filter media.

Acid-base components (γ_i^{AB}, γ_i^+ and γ_i^-) of the coal samples and dewatering aids were determined to better understand the mechanisms of the reagent adsorptions. The test results obtained using contact angle measurements indicated that the coal samples had mostly basic characteristics, while many of the reagents had acidic characteristics. The dewatering test results showed that when the acidic reagents were used on the basic coal surface as dewatering aids, the moisture reduction of these reagents were higher than that of the basic reagent. In addition to the van der Waals, electrostatic and hydrophobic forces, it is possible to conclude that there can be an acid-base interaction between the surface and the surfactant for the reagent adsorptions.

It is reported that there is a relationship between surface hydrophobicity, work of cohesion *Wc*, work of adhesion *Wa* and surface free energy ΔG of the system. As known,

hydrophobicity of the solid becomes dominant when the work of cohesion is higher than that of the adhesion. The work of adhesion can also be associated with the acid-base interaction γ_s^{AB} in water. Adding surfactant to the surface makes the Wc larger for the improvements of surface hydrophobicity and, hence, dewatering fines.

In order to determine the surfactant layer on a hydrophobic surface, a silica plate was coated using LPD, and then performed for LB tests. The LB test results with Span 80 (33.3% in diesel) showed that there was no monolayer formation on the carbon surface, which may be attributed to the diesel molecules presented in the surfactant. However, the contact angle measurements indicated that the contact angel was increased on the plate, which means that the surface was covered by the surfactant molecules.

A possible parameter that needs to be considered is the surface forces of the particle surface in the presence and absence of the dewatering aids. For this reason, AFM tests were conducted on the glass sphere and silica plate using electrolytes and chemicals. In the first tests, electrolyte addition decreased the repulsive force, which is desired for the coagulation of the fine particles. The later tests were done in three steps at 40-45 °C: the first one was with no chemical, the second was with low dosages of DAHCl and the third was with the amine and a dewatering aid together. The test results showed that the hydrophobic force was exponentially improved by the surfactant addition on the sample surface. Therefore, the hydrophobic improvements can be the reason for the high moisture reduction of the cakes obtained in this study.

The dewatering kinetic tests were conducted on the Pittsburgh, Elkview and West Virginia DMC sample in the presence and absence of dewatering aids. The kinetic test results disclosed that the line slopes of each dewatering test and position of the lines were changed. In the first case, the reagent addition caused the lines to lower in slope, which could be attributed to the fact that the cake became more permeable with the reagents. In the second case, the surfactant addition decreased interception of the lines, which means that medium resistance was also decreased probably due to the hydrophobic coagulation. Not only that, the kinetics data also shows that in the presence of dewatering aids the contact angle, surface tension, cake resistance, breakthrough pressure and cake formation time were exponentially changed, which is the desired conclusion for the dewatering process of the present work.

REFERENCE

1. Cunch, G.R., Advanced Coal Cleaning Technology, IEA Coal Research/44, London, UK, V.81, December 1991
2. Yoon, RH., Luttrell, G.H., USA Patent No: 5,458,786, October 17, 1995
3. Gray, V.R., "The Dewatering of Fine Coal," J. Inst. Fuel, Vol. 31, p.96-108, 1958.
4. Leonard, III, J.W., `Coal Preparation, Fifth Edition`, Society for Mining, Metallurgy, and Exploration, Inc., Littleton – Colorado, 1991
5. Svarovsky, B., `Solid-liquid Separation, Second Edition, London, 1991
6. Baker, A.F., Hot Surfactant Solution as a Dewatering Aid During Filtration. In Symposium of Coal Preparation, p.175, October 1976.
7. Gala, H. Dewatering and Drying of Ultrafine Coal - An Overview of Recent Research Activities,p.1, December 1989.
8. Ranjan, S., Hogg, R. The Role of Cake Structure in the Dewatering of Fine Coal by Filtration. Coal Preparation, V. 17, p.71, 1996.
9. Basim B.G., and Yoon, R.H., `Dewatering Fine Coal Using Novel Methods`, SME Annual Meeting, Orlando – Florida, March 9-11 1998
10. Wills, B.A., `Mineral Processing Technology, 5th Edition`, Pergmon Press, New York, 1992
11. Shaw DJ., `Introduction to Colloid and Surface Chemistry`, Butterworth-Heinemann ltd., USA 1992
12. Singh, B.P., "The Influence of Surface Phenomena on the Dewatering of Fine Clean Coal," Filtration and Separation, March, 1997, pp.159-163.
13. Osborne D.G., `Solid - Liquid Separation, Chapter 10, Volume 1`, Coal Preparation Technology, Indonesia, 1988
14. Leja, J. Surface Chemistry of Froth Flotation. Plenium Press, 1982.
15. Myers D. Surfactant Science and Technology. VCH Publishers, 1988.
16. Fuerstenau, M.C., `Flotation, Volume 1`, Society of Mining Society, New York, 1976
17. van Oss, C.J. Interfacial Forces in Aqueous Media. Marcel Dekker, inc., New York., 1994,
18. Adamson, A.W, and Gast, A.P. Physical Chemistry of Surfaces – sixth addition. John Wiley & Sons, inc, New York 1997,

19. Fieser L.F., and Fieser M., `Organic Chemistry, 3rd Edition`, Chapman & Hall, Ltd, London, 1956
20. Atkins, P. Physical Chemistry – sixth addition. W.H. Freeman and Company, New York, 1998
21. Davies, J.T. and Rideal, E.K., `Interfacial Phenomena` 2nd edition, Academic Press, 1963
22. Yoon, RH. and Basilio, C.I. USA Patent No: 5,670,056, September 23, 1997
23. Bancroft, W.D., `Applied Colloid Science`, McGraw-Hill, New York, 1932,
24. Ososkov, V.K., Ovsyannikova, N.N., Kornelli, M.E., and Pirgo, S.A., `Effect of temperature on the process of flotation separation of emulsified petroleum products`, Soviet Journal of water chemistry and technology, Vol. 8, No. 3, 1986, pp.83-84
25. Zettlemoyer, A.C., Ind. Eng. Chem., 57, 27(1965)
26. Rogers, M.G., A computer model for vacuum filter operation, Proceedings of dewatering technology & Practice Conference, Brisbane – Australia, 1989, pp. 99-104
27. Tiller, F. M. and Crump, J.R. Solid-Liquid Separation: An Overview. Chemical Engineering Progress V. 65, p.65, 197,
28. Wakeman, R.J., International Journal of Mineral Processing, **3**, pp. 193-176, 1976
29. Wakeman, R.J., International Journal of Mineral Processing, **5**, pp.395-405, 1979
30. Tarleton, E.S., and Wakeman, R.J., Filtration and Separation, pp. 393-397, June 1994
31. Wakeman, R.J., Filtration and Separation, pp. 655-669, Nov/Dec. 1979
32. Wakeman, R.J., Trans IchemE, Vol. 56, 1978
33. Wakeman, R.J., Filtration and Separation, pp. 337 – 341, April 1995
34. Wakeman, R.J., Thuraisingham, S.T., and Tarleton, E.S., Filtration and Separation, pp. 277-283, July/August 1989
35. Wakeman, R.J., and Tarleton, E.S., Filtration and Separation, Nov/Dec., pp. 412-419, 1990
36. Walker, A.J., and Svarovsky, L., Filtration and Separation, January/February 1994, 31(1), pp.57-65
37. Carman, P.C., Solid Science, 52:10, 1941
38. Darcy, H.P.G., `Les Fontains Publique de la Ville de Dijon`, Victor Dalmont, Paris, 1856
39. Condie, DJ., Hinkel, M., and Veal, C.J., `Modeling the Vacuum Filtration of Fine Coal`, Filtration and Separation, October 1996, Page 825-833

40. Condie, DJ., and Veal, C.J., `Modeling the Vacuum Filtration of Fine Coal: Part 2`, Filtration and Separation, November 1997, Page 9-16
41. Carleton, A.J. and Mackay, D.J., `Assessment of models for predicting the dewatering of filter cakes by gas blowing`, Filtration and Separation, May/June 1988, 25 (3), pp. 187-191
42. Yoon, RH. and Basilio, C.I. USA Patent No: 5,670,056, September 23, 1997
43. Aplan, F.F., `Properties dictate coal flotation strategies`, Mining Engineering, Jan. 1993, pp. 83-96
44. Sing, P., Filtration and Separation, March 1977, pp.159-163
45. Moudgil, B.M., and Scheiner, B.J., `Flocculation and Dewatering`, United Engineering Trustees, Inc., 1989
46. Meenan, G.F., Proceedings of the Industrial Practice of Fine Coal Processing, Society of Mining Engineering, 1988, pp. 223-229
47. Kural, O., `Coal, Resources, Properties, Utilization, Pollution`, Istanbul – Turkey, 1994
48. Kural, O.,` Komur, Ozellikleri, Teknolojisi ve Cevre Iliskileri`, Istanbul-Turkey, 1998
49. Carman, P.C., "Fluid Flow through Granular Beds," Trans. Ins. Chem. Eng., Vol. 15., pp. 150-166, 1937.
50. Aksoy, B.S., "Hydrophobic Forces in Free Thin Films of Water in the Presence and Absence of Surfactants," Ph.D. Thesis, 1997
51. Hosten, C., Filtration Behavior of Finely Ground Hematite Slurries`, Ph.D. Thesis, University of California, Berkeley, 1982
52. Groppo JG., Parekh B., `Surface Chemical Control of Ultra-fine Coal to Improve Dewatering`, Coal Preparation a Multinational Journal, USA, 1996
53. Dzinomva G. P. T., Wood, C. J. Superabsorbent Polymers for the Dewatering of Fine Coal. Seventh Australian Coal Preparation Conference, p.200, 1995.
54. Gerl, S., Stahl, W. Improved Dewatering of Coal by Steam Pressure Filtration. Coal Preparation, V. 17, p.137, 1996
55. Tosunoglu, I., Sahinoglu, S. On the Constancy of Average Porosity in Filtration. The ChemicalEngineering Journal V.34, p.99, 1987
56. Israelachvili, J., and Pashly, R.M., Nature 300 (1982), 341

57. Israelachvili, J., and Pashly, R.M., Journal of Colloid and Interface Science, **98**, No: 2, 1984
58. Ducker, W.A., Senden, T.J., and Pashly, R.M., Langmuir, **8**, 1831, 1992
59. Zisman, W.A., Chapter 3 in Handbook of Adhesion, Ed. Van Nostrad., New York, 1977
60. Hiemenz, P.C., and Rajagopalan, R., Principles of colloids and surface chemistry, 3rd Edition, Marcel Dekker, Inc., 1997
61. Rabinovich, Y.I., and Yoon, R.H., Colloids and Surfaces, **93**, 263, 1994
62. Yoon, R.H., Advances in Flotation Technology, Eds. Parekh, B.K., and Miller, J.D., SME Inc., 1999
63. Pazhianur, R., and Yoon, R.H., SME Meeting, Salt Lake City, 2000
64. Yoon, R.H., and Ravishankar, S.A., J. Colloid Interface Sci., 179 (1996), 361
65. Flinn, D.H., Guzonas, D.A., and Yoon, R.H., J. Colloids and Surf. 87 (1994), 163
66. Aksoy, S.B., and Yoon, R.H., J. Colloid Interface Science, 1999
67. Pazhianur, R., `Hydrophobic Forces in Flotation` PhD. Thesis at Virginia Tech, VA-USA, 1999,
68. Vivek, S., `Effects of long-chain surfactants, short-chain alcohols and hydrolyzable cations on the Hydrophobic and Hydration Forces`, Ph.D. Thesis at VT, 1998
69. Honaker, R.Q., `A fundamental study of the selective hydrophobic coagulation process`, Ph.D. Thesis at VT, 1992
70. Fowkes, F.M., J. Phys. Chem., 66 (1962), 682
71. Zisman, W.A, Ind. Eng. Chem., 55 (1963), 19
72. Laskowski, J.S., and Kitchener, J.A., J. Colloid Interface Sci., 29 (1969), 670
73. Van Oss, C.J., Good, R.J., and Chaudhary, M.K., Chem Rev., 88 (1988), 927
74. Israelachvili, J., `Intermolecular and Surface Forces, 2nd Edition`, Academic Press, 1992
75. Yoon, R.H., `Role of hydrodynamic and surface forces in bubble-particle interaction`, Int. J. Miner. Process., 58 (2000) 129-143
76. Cheremisinoff, N. P., Azbel, D. S. Liquid Filtration. Ann Arbor Science, 1983. V.17, p. 137, 1996.
77. Matteson, M.J., Filtration, Principles and Practice, 2nd Ed., Chemical Industries/27, 1987
78. Sis, H., and Chander, S., `Pressure filtration of dispersed and flocculated Alumina Slurries`, SME Meeting, Orlando-Florida, March 9-11, 1998

79. Bhattacharya, I.N., Settling and filtration characteristics of fine alumina trihydrate slurry`, Int. J., Miner. Process., 49(1997) 107-118
80. Willis, M.S., Tosun, I., `A rigorous cake filtration Theory`, Chemical Eng. Sci., 34 (1980) 2427-2438
81. Holdich, R.G., Filtration and Separation, Nov./Dec., 1990,435-439
82. Weise, N.L., SME Mineral Processing Handbook, Volume 1`, 1985, pp.9-14
83. Bourgeois, F.S., and Barton, W.A., `Advances in the fundamentals of fine coal filtration`, Coal Preparation, Vol. 19, 1998, pp. 9-31
84. Hosten, C., and Sastry, K.V.S., Mineral Eng., Vol. 2, No: 1, 1989, pp.111-119
85. Walker, A.J., and Svarovsky, L., Filtration and Separation, Jan./Feb., 1994, pp.57-65
86. Green, P. Dewatering of Coal and Refuse. Coal Age, V. 86, p.145, 1981
87. Rushton, A., Ward, A.S., and Holdich, R.G., `Solid-Liquid Filtration and Separation Technology`, VCH, New York, 1996
88. Owen, M. J. In Interfacial Phenomena in Coal Technology (eds. G. D. Botsaris and Y. M. Glazman), Surfactant science series, V. 32, p.157, 1988.
89. Ruberto, R. G. and Cronauer, D. C. In Organic Chemistry of Coal (ed. J. W. Larsen), ACS Symposium Series 71, Washington D. C., 1978, p.50.
90. Veal, C.J., `Improving the vacuum filtration of fine coal using simultaneous dewatering and size enlargement`, AFS, Volume 2, 1997, pp.541-546
91. Kosman, J.J., and Rowell, R.L., `Surfactant binding and the electrophilicity of coal`, Colloids and Surfaces, 4(1982) 245-254
92. Sung, D.J., Kang, S.H., and Parekh, B.K., `Evaluation of hyperbaric filtration for fine coal dewatering: Part 2. Effects of chemical addition`, AFS, 1996, pp. 480-488
93. Xu, Z., `Study of Hydrophobic Interaction in Fine Particle Coagulation`, PhD. Thesis at Virginia Tech, VA-USA, 1990
94. Good, R.J., Srivates, N.R., Islam, M., Huang H.T.L. and van Oss, C.J. Theory of the acid-base hydrogen bonding interactions, contact angle, and the hysteresis of wetting: application to coal and graphite surface. J. Adhesion Sci. Technol. Vol. 4. No 8, 1990, pp. 607-617
95. Van Oss, C.J. and Giese R.F. The Hydrophilicity and Hydrophobiciy of the Clay Minerals. Clays and Clay Minerals, Vol. 43, No. 4, pp. 474-477, 1995,

96. Joslin, S.T., Fowkes, F.M. (1985), Surface Acidity of Ferric Oxides Studied by Flow Microcalorimetry. Ind. Eng. Chem. Prod. Res. Dev., Vol. 24, pp 369-375
97. Fowkes, F.M., Jones, K.L., Li, G., and Lloyd, T.B., `Surface chemistry of coal by flow microcalorimetry`, Energy and Fuels, 3 (1989), 97-105
98. Bourgeois, F.S., and Lyman, G.J., Morphological analysis and modeling of fine coal filter cake microstructure`, Chemical Engineering Sci., Vol. 52, No. 7, 1997, pp.1151-1162
99. Michalski, M.C., Hardy J., and Saramago B.J.V., On the Surface Free Energy of PVC/EVA Polymer Blends: Comparison of Different Calculation Methods. Journal of Colloid and Interface Science, Vol. 208, 1998, pp. 319-328
100. Laskowski, J.S. Oil assisted fine particle processing. Colloid Chemistry in Mineral Processing (Eds. J.S. Laskowski and J. Ralston). Elsevier Publisher, New York, 1992
101. van Oss, C.J., and Good, R.J., On the Mechanism of Hydrophobic Interaction. J. Disp. Science and Tech. Vol. 9, 1988, pp.355-362
102. Schultz, J., and Nardin, M., Determination of the Surface Energy of Solids by the Two-Liquid-Phase Method. Modern Approaches to Wettability – Theory and Application (Eds. Schrader and Leob), Plenum Press, New York, 1992 pp. 73-100.
103. van Oss, C.J., Giese, R.F., and Wu, W., On the Predominant Electron-Donicity of Polar Surfaces. J. Adhesion, Vol. 63., 1997, pp. 71-88,
104. Phillips, K.M., Glanville, J.O., and Wightman, J.P., `Heat of immersion of Virginia-C coal in water as a function of surface oxidation`, Colloids and Surfaces, 21(1986) 1-8
105. Grzybek, T. and Kreiner, K. Surface Changes in Coals after Oxidation. 1. X-ray Photoelectron Spectroscopy Studies. Langmiur V.13, p. 909, 1997.
106. Keller, D. V., Stelma, G. J., and Chi, Y. M. Surface Phenomena in the Dewatering of Coal.
107. Harris, C. C., Smith H. G. The Moisture Retention Properties of Fine Coal: Part 1. Second Symposium of Coal Preparation, University of Leeds, p. 57, October 1957.
108. Parfitt, G. D., and Sing, S. W. Characterization of Powder Surfaces, Academic Press, London, 1976.

109. Gray, V. R. The Dewatering of Fine Coal. Journal of the Institute of Fuel V.31, p.96, 1958.

110. Silverblatt, C. E., Dahlstrom, D.A. Moisture Content of a Fine-Coal Filter Cake. Industrial and Engineering Chemistry, V. 46, p.1201, 1954.

111. Smith, G. R. S. Filter Aids. In Solid-Liquid Separation. (Ed. L. Suarowsky), p.265, 1985.

112. Veal, C. J., Jonston, B. K., Nicol, S. K. The Potential of Gas Purging for the Reduction of Coal Moisture. Seventh Australian Coal Preparation Conference, p. 158, 1995.

113. Phillips, J. W., Thomas, D. G. A. Removal of Water From Fine Coal. Colliery Engineering V.32, p.15, 1955.

114. Theliander H. and Fathi-Najafi, M. Simulation of Build-up of a Filter Cake. Filtration & Separation, V.33 , p.417, May 1996.

115. Stelma, G. J. Influence of Surfactants on the Dewatering of Coal. Syracuse University, Ph.D. Thesis, 1978.

116. Sung, D. J., Groppo, J. G., Parekh, B. K. Cake Uniformity in Pressure Filtration of Coal Slurry. Filtration and Separation, V. 31, p.819, December 1994

117. Celik, M.S., and Somasundran, P., `Effects of pertreatments on flotation and electrokinetic properties of coal`, Colloids and Surfaces, 1(1980) 121-124

118. Grace H.P., `Resistance and Compressibility of Filter Cake, Part III. Under Conditions of Centrifugal Filtration`, in Chemical Engineering Progress, Vol. 49, No. 8, August 1953, pp 428-436

119. Dahlstrom, D.A., `Fundamentals of Solid-Liquid Separation`, Design and Installation of Concentration and Dewatering Circuits, 1986, pp 103-114

120. Samuel, W.S., Morris, L.E. USA Paten No: 4,210,531, July 1, 1980

121. Donald, R.C., USA Patent No: 5,256,169, October 26, 1993

122. Roger. N.E., Joseph, P.J., Roderick, R.G., USA Patent No: 5,405,554, April 15, 1995

123. Fuerstenau, M.C., `Flotation, Volume 2`, Society of Mining Society, New York, 1976

124. Lockhart NC., Veal CJ., `Coal Dewatering: Australian R&D Trends`, Coal Preparation a Multinational Journal, USA, 1996

125. Weston, VJ., Slottee JS., `Recessed and Membrane Plate Pressure Filter Application to Mineral Concentrate and Other Rapid Filtering Material`, Advances in Filtration and Separation Technology, Utah-USA, 1991.

126. Keller, K., and Stahl, W., `Vibration Dewatering`, Chemical Engineering and Processing, 33 (1994) 331-336

127. Keller, K., and Stahl, W., `Enhanced solid-liquid separation by using combination of vibration and capillary suction`, ASF, 572-577

128. Pearce K.W., `Effects of Improving Vibrations on Filtration`, Filtration & Separation, July/August, 1986, pp.220-222

129. Brownell, L. E., Katz, D. L. Flow of Fluids Through Porous Media. Chemical Engineering Progress V. 43, p. 573, p.601, 1947,

130. Ruth, B., Studies in Filtration, III. Derivation of general filtration equation, IV. Ind. Eng. Chem., 1933, 27, pp. 708-806

131. Nicolaous, I. and Stahl, W., Calculation of rotary filter plants, Auf. Tech., 1992, 33, pp. 328-338

132. Kenney, Mark E. USA Patent No: 5,346,630, March 15, 1993